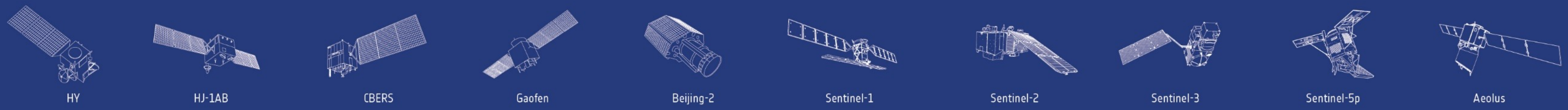

2023 DRAGON 5 SYMPOSIUM

3rd YEAR RESULTS REPORTING

11-15 SEPTEMBER 2023

[PROJECT ID. 59358]

[CHINA-ESA FOREST OBSERVATION]

<INSERT DAY & DATE IN PROGRAMME>

ID. 59358

PROJECT TITLE: CHINA-ESA FOREST OBSERVATION

PRINCIPAL INVESTIGATORS: PANG YONG, JUAN SUÁREZ

CO-AUTHORS: [PANG YONG, JUAN SUÁREZ, JAMES HITCHCOCK, GERRARD ENGLISH, DU LIMING, JIA WEN, ANTONY WALKER, JACQUELINE ROSETTE, LI ZENGYUAN, LI SHIMING, MENG SHILI, NIU XIAODONG, YU TAO, LIANG XIAOJUN, YAN MING, LV QIAN]

PRESENTED BY: PANG YONG, JUAN SUÁREZ

Dragon 5 3rd Year Results Reporting

- Inform on the project's objectives
- Detail the Copernicus Sentinels, ESA, Chinese and ESA Third Party Mission data utilised after 3 years
- Detail the in-situ data measurements and requirements
- Provide details on field data collection campaigns and periods in P.R. China or other study areas
- Inform on the results after 3 years of activity
- Inform on the project's schedule, planning & contribution of the partners for the following year
- Report on the level and training of young scientists on the project achievements, including plans for academic exchanges
- Report on the peer reviewed publications (nr. of papers, journal name and publication title) after 3 years of activity

EO Data Delivery

Data access (list all missions and issues if any). NB. in the tables please insert cumulative figures (since July 2020) for no. of scenes of high bit rate data (e.g. S1 100 scenes). If data delivery is low bit rate by ftp, insert "ftp"

ESA /Copernicus Missions	No. Scenes
1. Sentinel-2A/B	380
2.	
3.	
4.	
5.	
6.	
Total:	380
Issues:	

ESA Third Party Missions	No. Scenes
1. Ladsat5, 7, 8	1988
2. PLANET	100
3.	
4.	
5.	
6.	
Total:	2088
Issues:	

Chinese EO data	No. Scenes
1. GF-2	16
2. GF-7 optical stereo images	2
3. GF-7 laser footprints	42
4. TECIS CASAL	67
5. TECIS stereo images	12
6. GF-6	21
Total:	160
Issues: A total of 575.9 km^2 airborne LiDAR data were used in Pu'er study area during 3 years.	

European Young scientists contributions in Dragon 5

Name	Institution	Poster title	Contribution including period of research
English Gerrard	Swansea University	Remotely Sensed Vegetation Indices Detect Differing Drought Responses Between Sitka spruce (Picea sitchensis) Genotypes	Calibration of stress VI
Hitchcock James Alan	Forest Research	Methods for assessing forest stress with satellite Remote Sensing	Time-series analysis of satellite imagery monitoring stress

Chinese Young scientists contributions in Dragon 5

Name	Institution	Poster title	Contribution including period of research
Liming Du	Institute of Forest Resource Information Techniques CAF	Potential Assessment of LBI for forest carbon sink measurement	Forest height estimation using GF-7, biomass estimation using airborne LiDAR
Wen Jia	Institute of Forest Resource Information Techniques CAF	Satellite Reflectance Validation based on BRDF Reconstructed Airborne Hyperspectral Data	hyperspectral RS for China-ESA satellite data evaluation
Tao Yu	Institute of Forest Resource Information Techniques CAF	An optimized method to validate high resolution gross primary production based on flux tower measurement	forest carbon flux parameter inversion and evaluation method using sentinel-2 data

System integration, multi-source LiDAR data acquisition and application

CAF-LiTHy:

Chinese Academy of Forestry's Lidar-Thermal-Hyperspectral Airborne Observation System

LiDAR scanner: Riegl VQ580-II			
Wavelength	1064 nm	Laser beam divergence	0.25 mrad
Laser pulse length	3 ns	Scan angle range	±35°
Maximum laser	2000 kHz	Maximun scanning speed Point density@1000 m	300 lines/s 30 pts/m^2
Echo intensity	15 / beam-forming	Vertical accuracy	0.02 m
Medium wave infrared (MWIR) camera : InfraTec ImageIR		**Long wave thermal infrared (LWIR)camera: InfraTec VarioCam HD**	
Wavelength	2.0-5.7μm	Wavelength	7.5-14μm
Spatial pixels	640 x 512	Spatial pixels	1024 x 768
Frame rate	106 Hz	Frame rate	30 Hz
Focal length	28.6mm	Focal length	11.1mm
FOV	33.8°	FOV	46.6°
Temperature resolution	0.02 k	Temperature resolution	0.02 k
Temperature range	-40-1500℃	Temperature range	-40-2000℃
Hyperspectral sensor: Specim Aisa FENIX1K			
Wavelength	380-2500 nm	Spatial pixels	1024
Focal length	18.1mm	Spectral resolution	4.5/12 nm
FOV	40°	Maximum bands	87-348/256
Frame rate	100 lines/s	Output	12/16 bits

System integration, multi-source LiDAR data acquisition and application

Flight in Pu’er, China
Jan 13, 2023

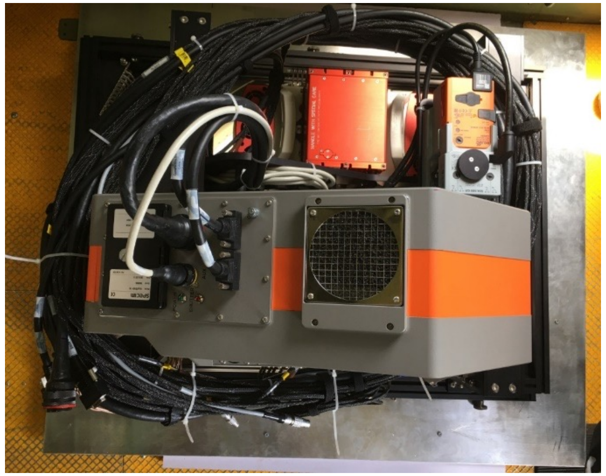

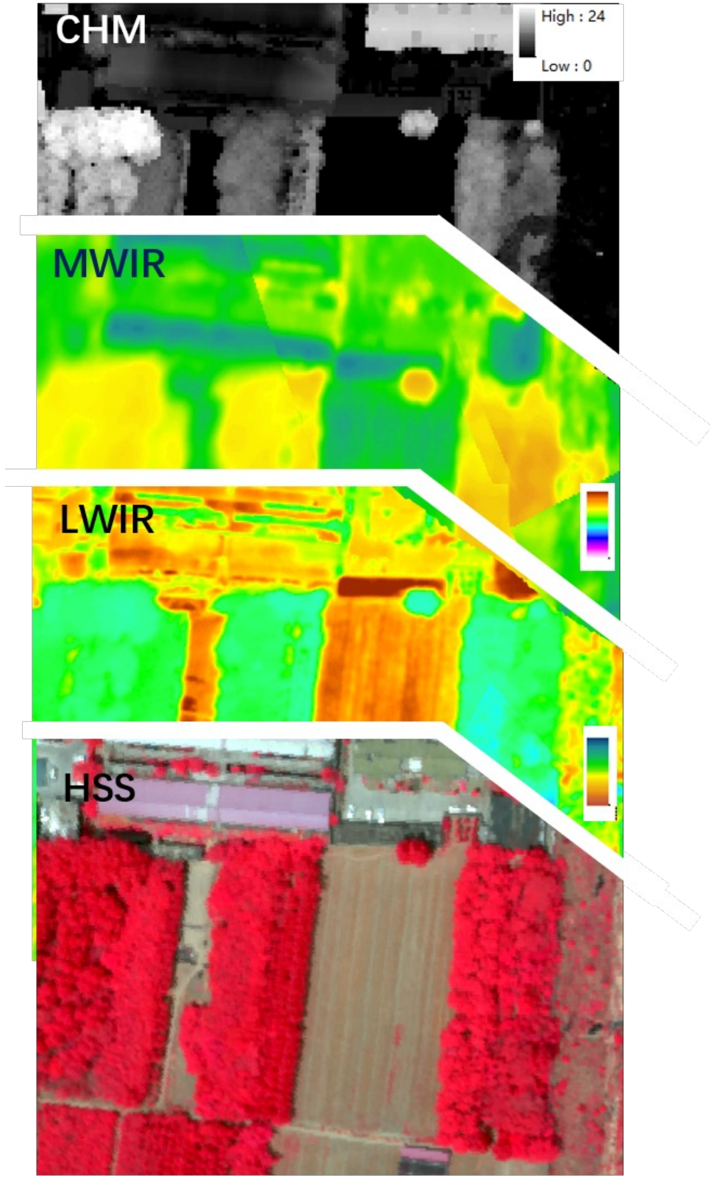

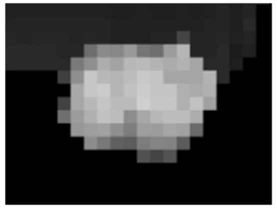

CHM image

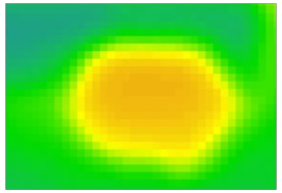

MWIR image

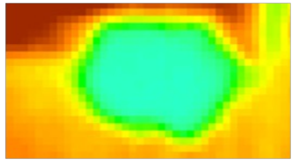

LWIR image

HSS image

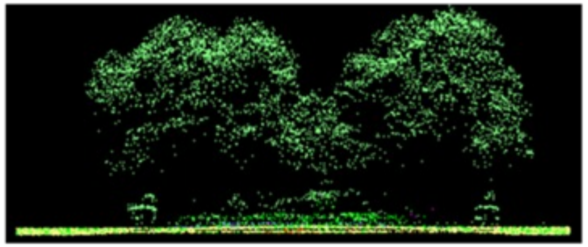

LiDAR pointcloud

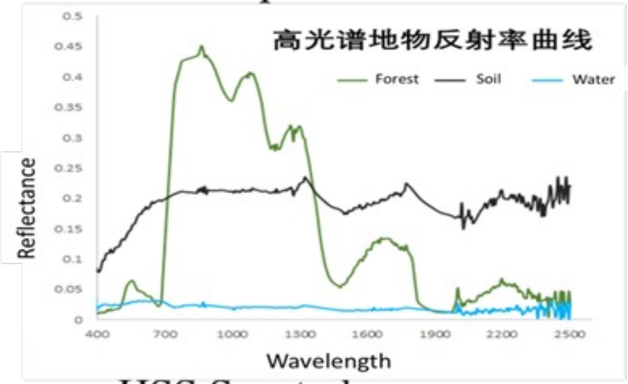

HSS Spectral curve

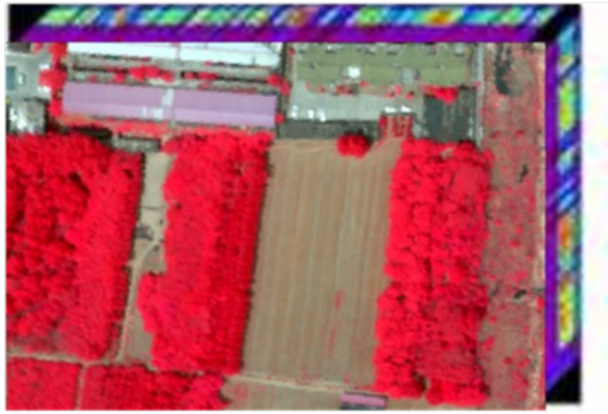

System integration, multi-source LiDAR data acquisition and application

- DEM, DSM, CHM of LiDAR

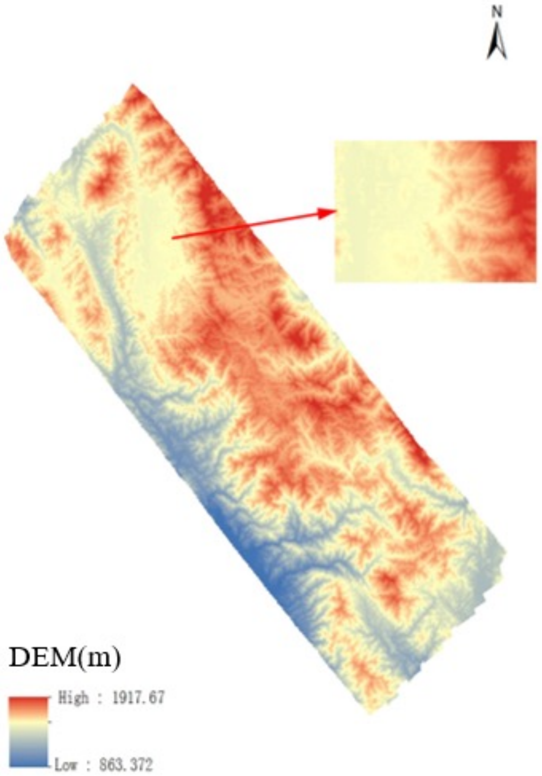

DEM

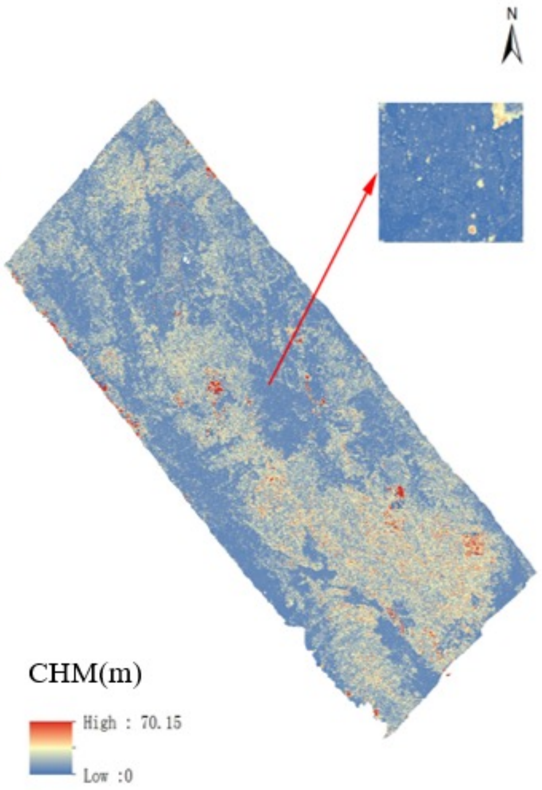

CHM

- Surface reflectance and NDVI of hyperspectral data

Surface reflectance

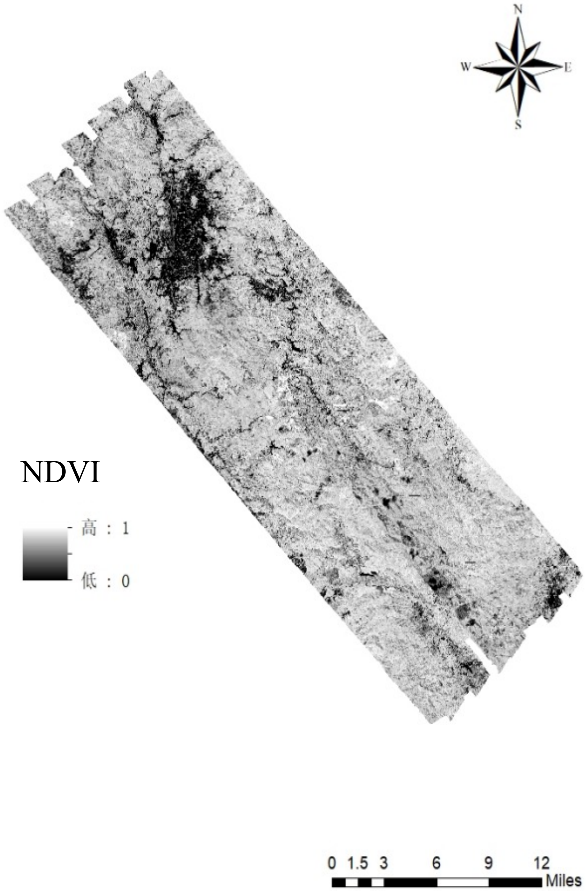

NDVI

The joint use of Chinese and European satellites

■ Pu'er forest cover mapping based on Sentinel-2 and GF-6 data

Research area and data:

- Sentinel-2 and GF-6 image data were respectively used for mapping.
- Field survey data, airborne data and terrain aid data were used.
- The results were compared with the existing land cover classification products, and the best scheme was selected for the forest cover type mapping in Pu 'er City.

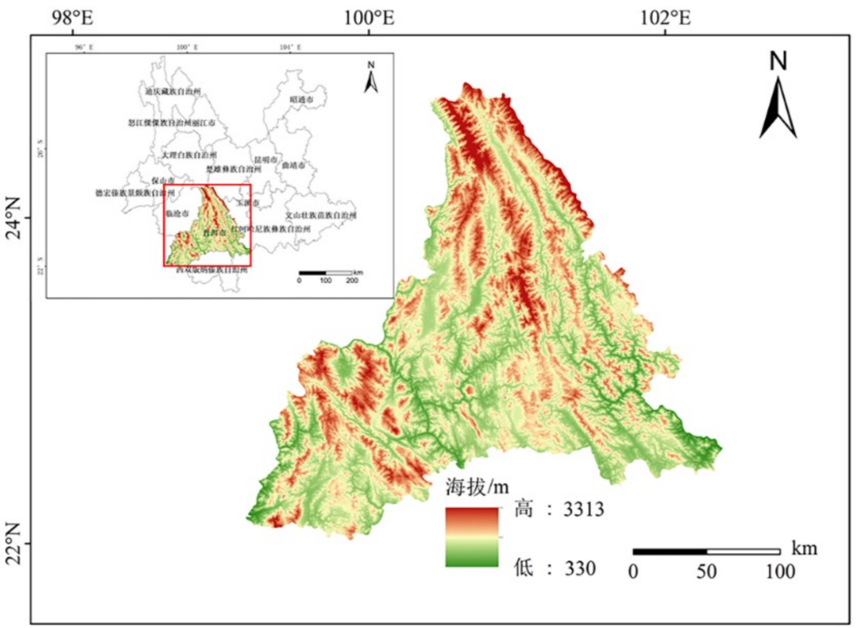

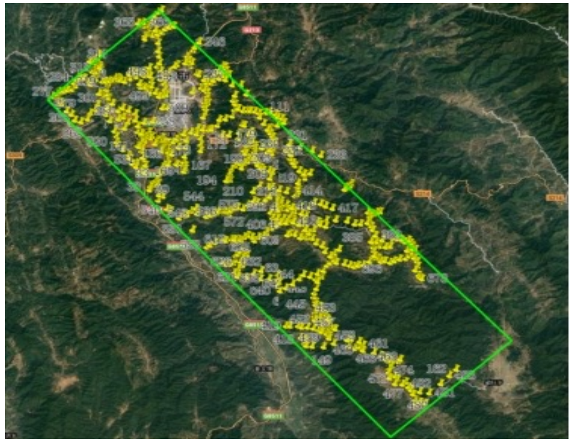

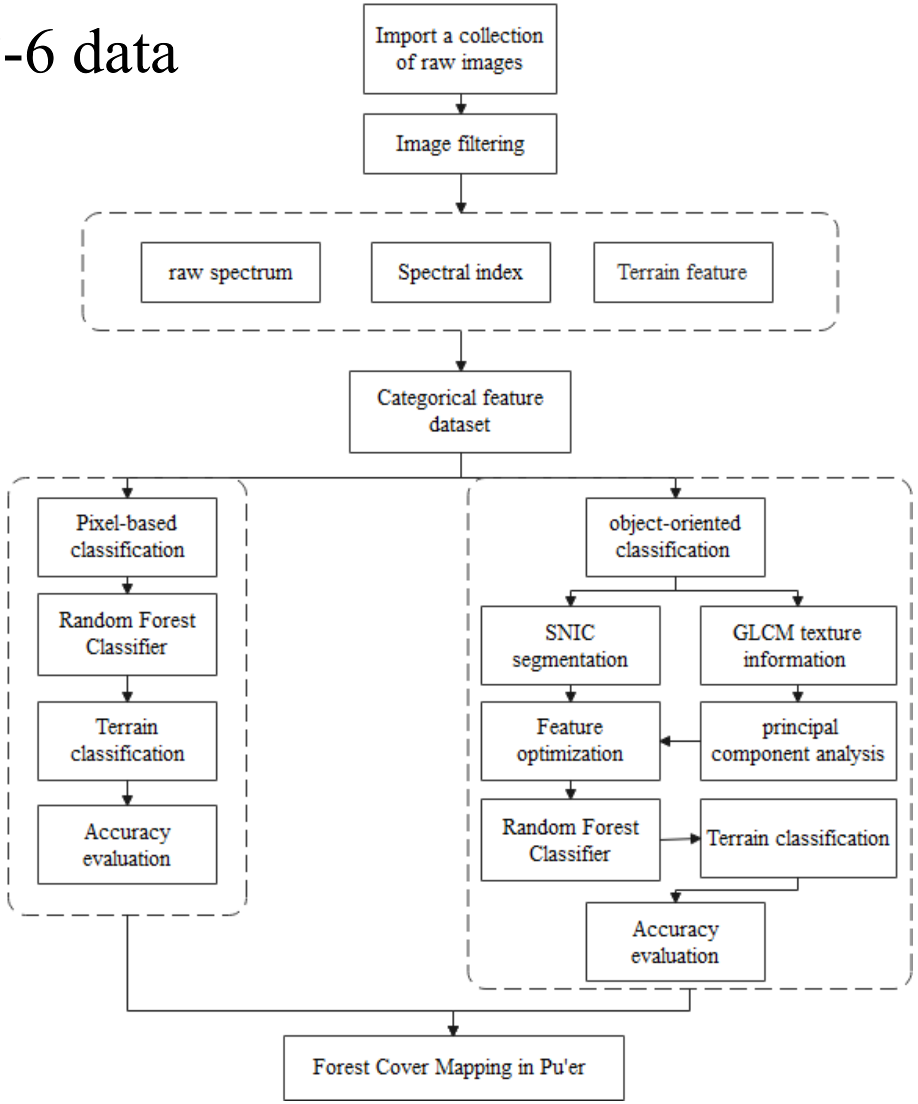

Forest Cover Remote Sensing Mapping Process

■ Pu'er forest cover mapping based on Sentinel-2 data

- The object-oriented method effectively reduce the "salt and pepper phenomenon" and improves the classification accuracy.
- Feature optimization avoids the influence of redundant information on classification results and improves classification efficiency.
- The results proves that the short-wave infrared band (B11, B12) and the near-infrared band (B8) play an important role in forest cover classification.

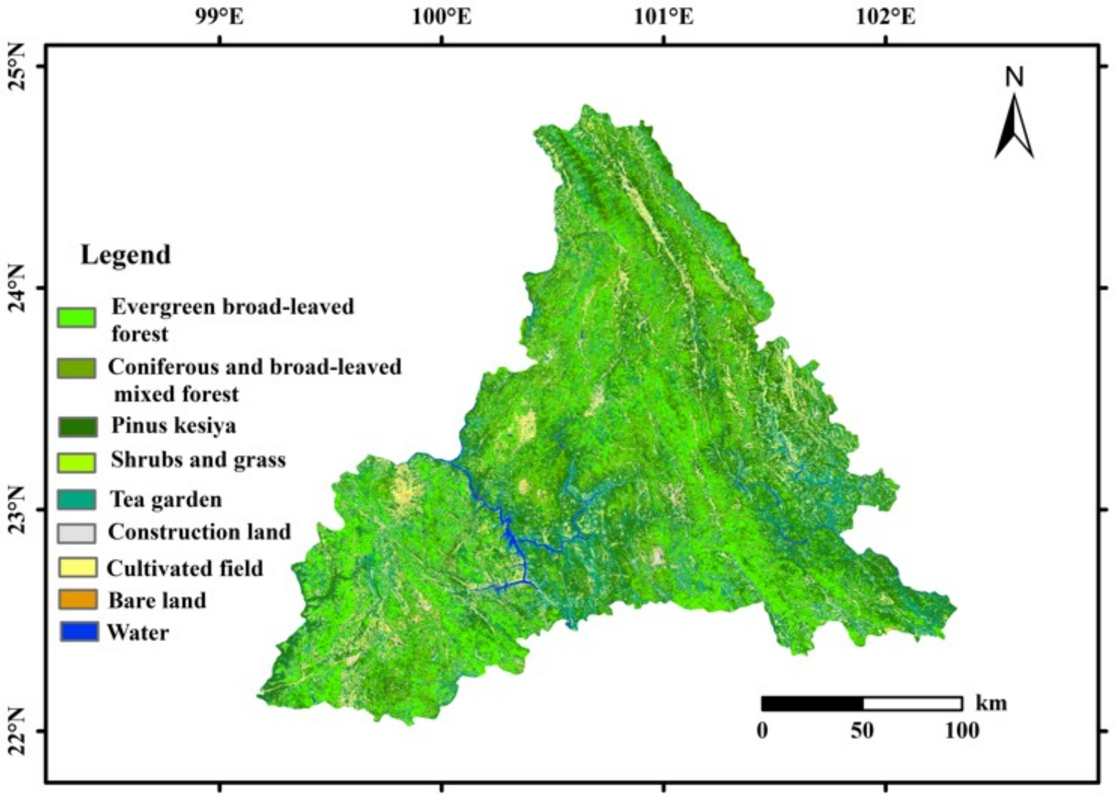

Classification thematic map

■ Pu'er forest cover mapping based on Sentinel-2 data

- **The overall accuracy of Pu'er LC data was the highest (86.96%), and the overall accuracy of the other three products was around 75%.**
- **In general, the four land cover products had high classification accuracy and reliability in Pu 'er.**

Accuracy evaluation result

Dataset	ESRI_Land_Cover_10m		ESA World Cover		Dynamic World		Pu'er LC	
	PA（%）	UA（%）	PA（%）	UA（%）	PA（%）	UA（%）	PA（%）	UA（%）
Forest	96.56	90.97	97.05	89.57	98.53	87.17	91.40	98.67
Shrub and grass land	57.89	45.45	42.11	44.94	33.33	38.75	66.32	58.88
Construction land	96.43	77.14	23.21	100.00	96.43	80.60	85.71	97.96
Cultivated field	35.87	66.00	68.48	74.12	42.86	66.10	86.96	71.43
Bare land	6.67	50.00	80.00	20.00	20.00	100	86.67	56.52
Water	75.00	100.00	42.50	100.00	82.50	100	92.50	100
OA（%）	80.28		76.60		79.91		86.96	
Kappa coefficient	0.673		0.611		0.656		0.796	

■ GF-7 LiDAR and stereo image for forest terrain and height estimation

Study area and data

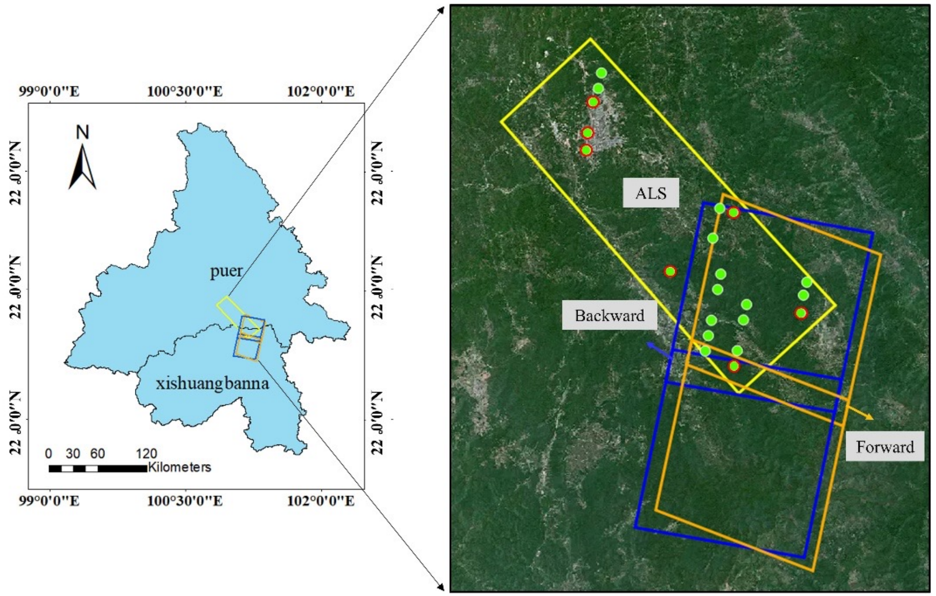

Pu’er study area

GF-7 stereo images and laser footprints

Two sets of stereo images which were obtained in the same orbit were acquired.

42 level 1A laser footprints covering the flight range of ALS data were obtained.

Airborne and UAV LiDAR data

Parameter	ALS	ULS
Sensor	Riegl VQ580- II laser scanner	DJI L1 laser scanner
Time	Dec 2020	Nov 2022
Point density	2-4 pts/m^2	300 pts/m2
CHM res	0.5 m	0.1 m

Forest inventory data

1726 sub-compartments in the overlap area of GF-7 stereo images and ALS data were utilized to evaluate the results.

■ GF-7 LiDAR and stereo image for forest terrain and height estimation

Terrain and canopy height estimation based on the effective laser footprints

25 effective footprints were used to measure the forest terrain, and 8 effective footprints were used to measure the forest height.

The distance between the starting position of the waveform signal and the ground return position was taken as the canopy top height;
The geodetic height calculated based on the laser echoes ranging value was taken as the ground elevation value of the laser footprint.

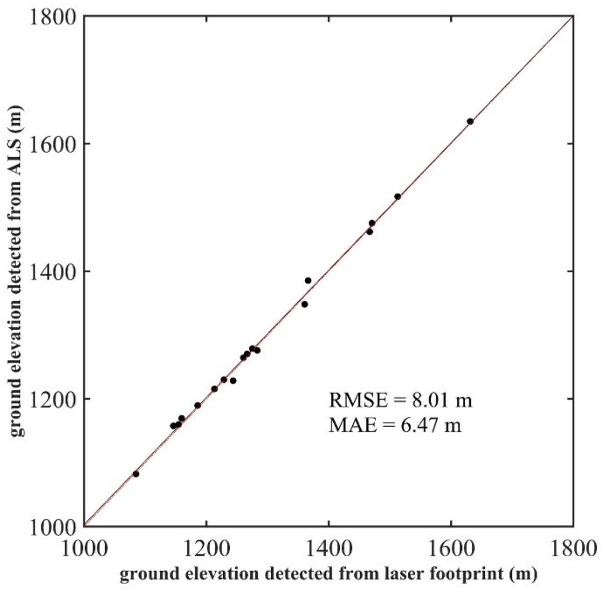

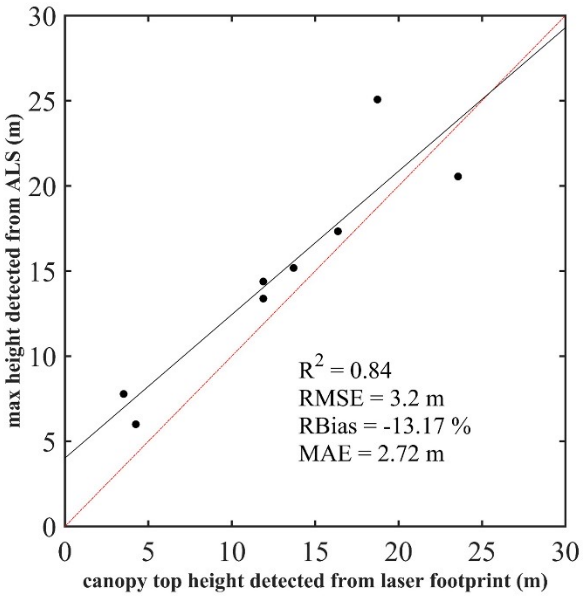

Regression of result detected from laser footprints and ALS point clouds

■ GF-7 LiDAR and stereo image for forest terrain and height estimation

Canopy height estimation based on stereo images and compared with ALS data

The CHM obtained from ALS point clouds was utilized to build the two scale reference data, and further applied to verify the canopy height calculated from the stereo images of GF-7.

Plot scale: the grid size is 20 m×20 m, and the corresponding mean height difference of each grid was calculated.

Forest stand scale: Each vector plane in the sub-compartment data was inward buffered 20 m and used to calculate the average height of the imaged-based CHM and ALS-based CHM.

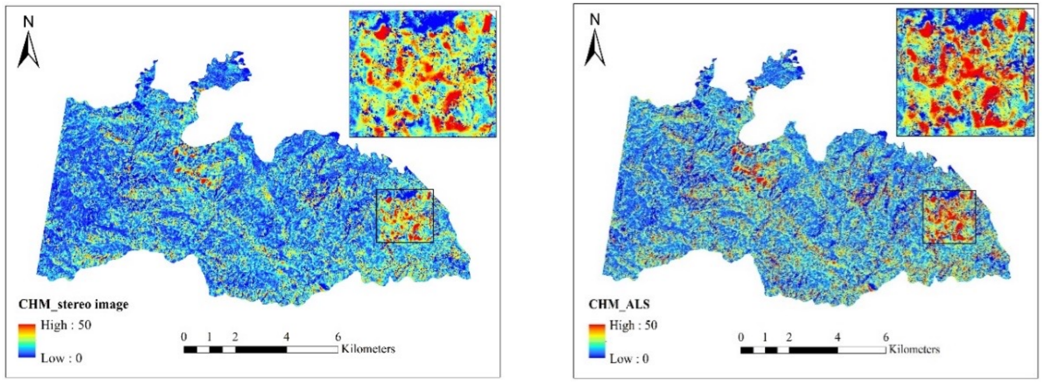

CHM obtained from GF-7 stereo images and ALS

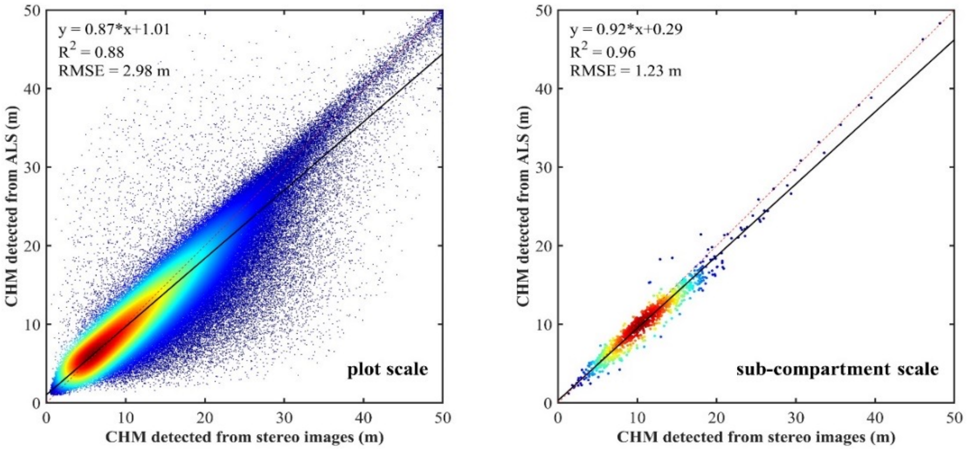

Regression result of CHM detected from stereo images and ALS data

■ GF-7 LiDAR and stereo image for forest terrain and height estimation

Canopy height estimation based on stereo images and compared with ULS data

The CHM obtained from ULS point clouds was utilized to build the plot scale reference data, and further applied to verify the canopy height calculated from the stereo images of GF-7.

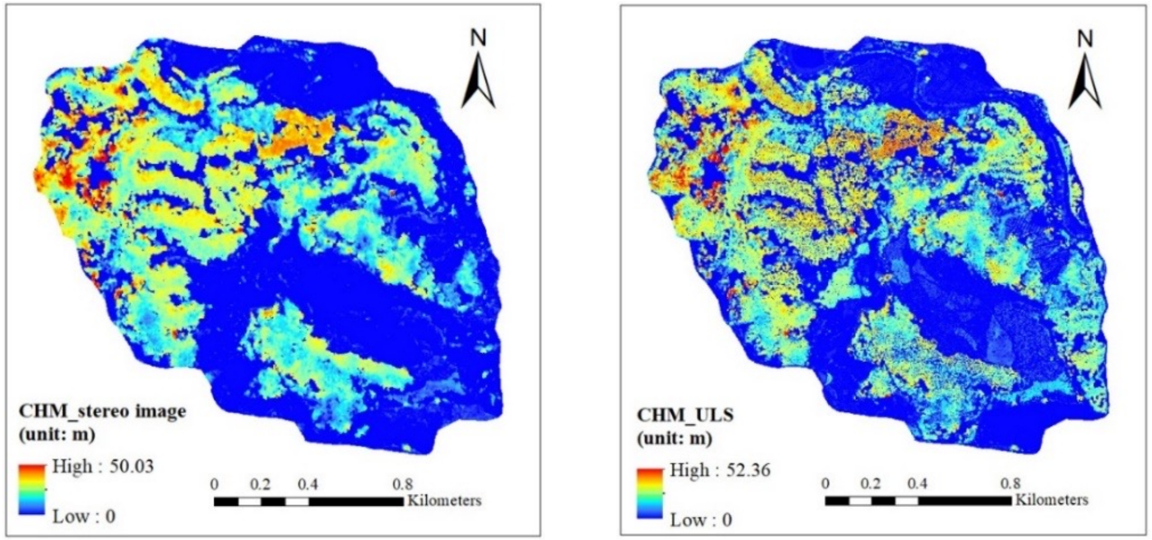

CHM obtained from GF-7 stereo images and ULS

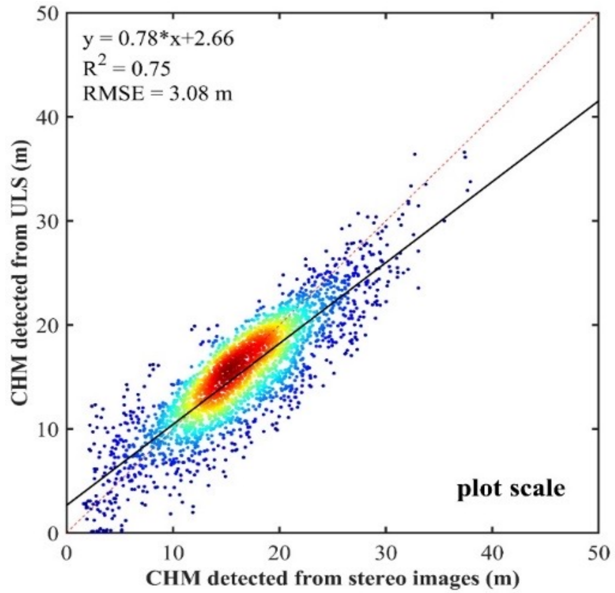

Regression result of CHM detected from GF-7 stereo images and ULS data

Brief introduction of Chinese TECIS

Launched on August 4th, 2022

Characteristics		Parameters		
CASAL	Beams	5		
	Repetition Frequency /Hz	40		
	Wavelength /nm	1064		
	Digitization Rate /GHz	1.2		
DMC	Observation angle /°	0	±19	±41
	Spectral Range /nm	450~520 520~590 630~690 770~890	450~520 520~590 630~690 770~890 500~760	450~520 520~590 630~690 770~890 690~730
	Spatial Resolution /m	2	4/8	6/12
	Swath width /km	20		
Orbit altitude	506 km			
Design Life	8 years			

■ Chinese TECIS data acquisition

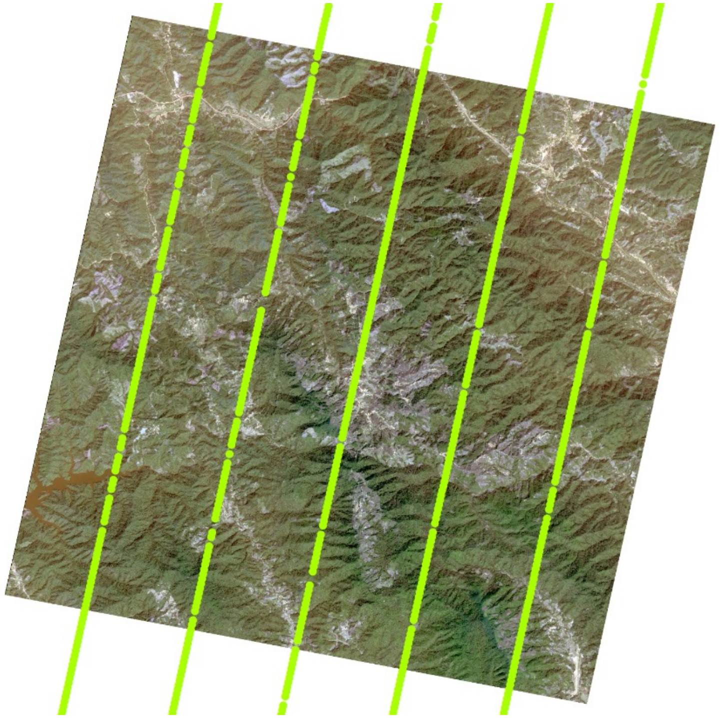

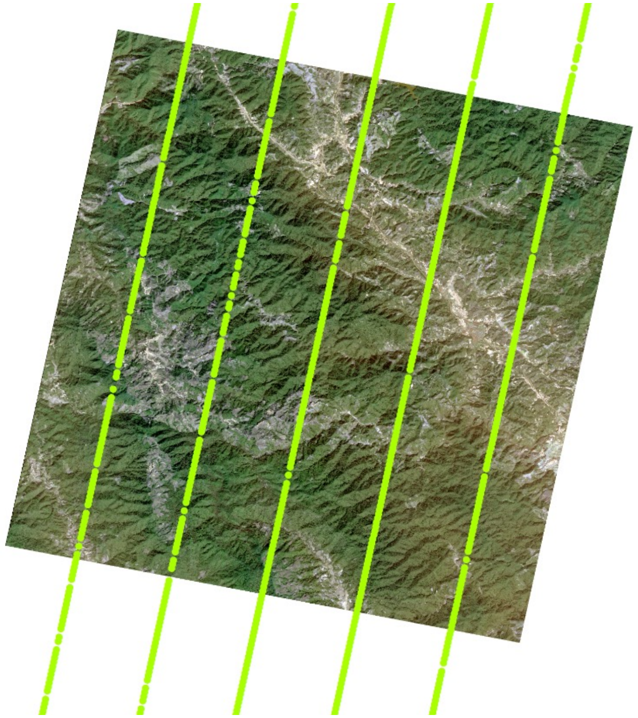

TECIS DMC image(cloud-free) NAD over CASAL footprints

The joint use of Chinese and European satellites

- Chinese TECIS data acquisition

Number of CASAL footprints： 0122(green): 27   0206 (blue): 40

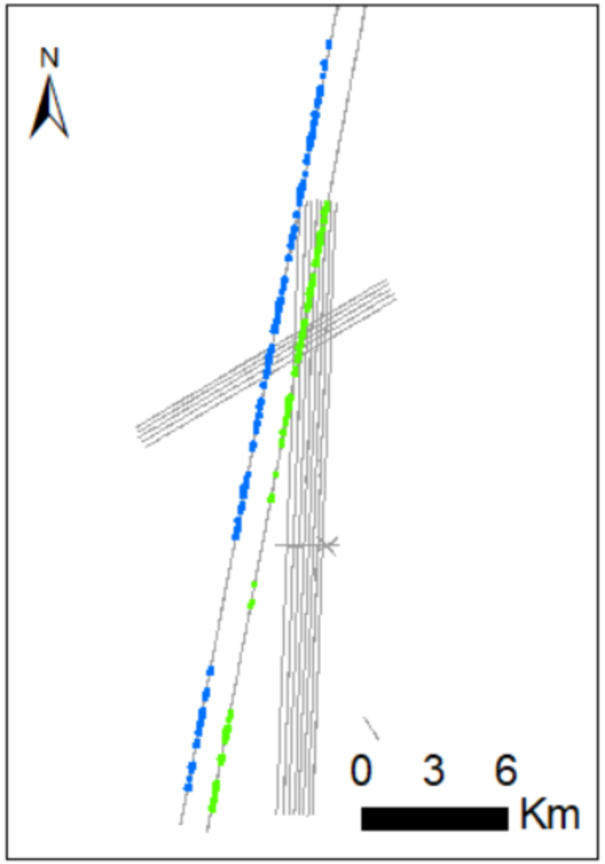

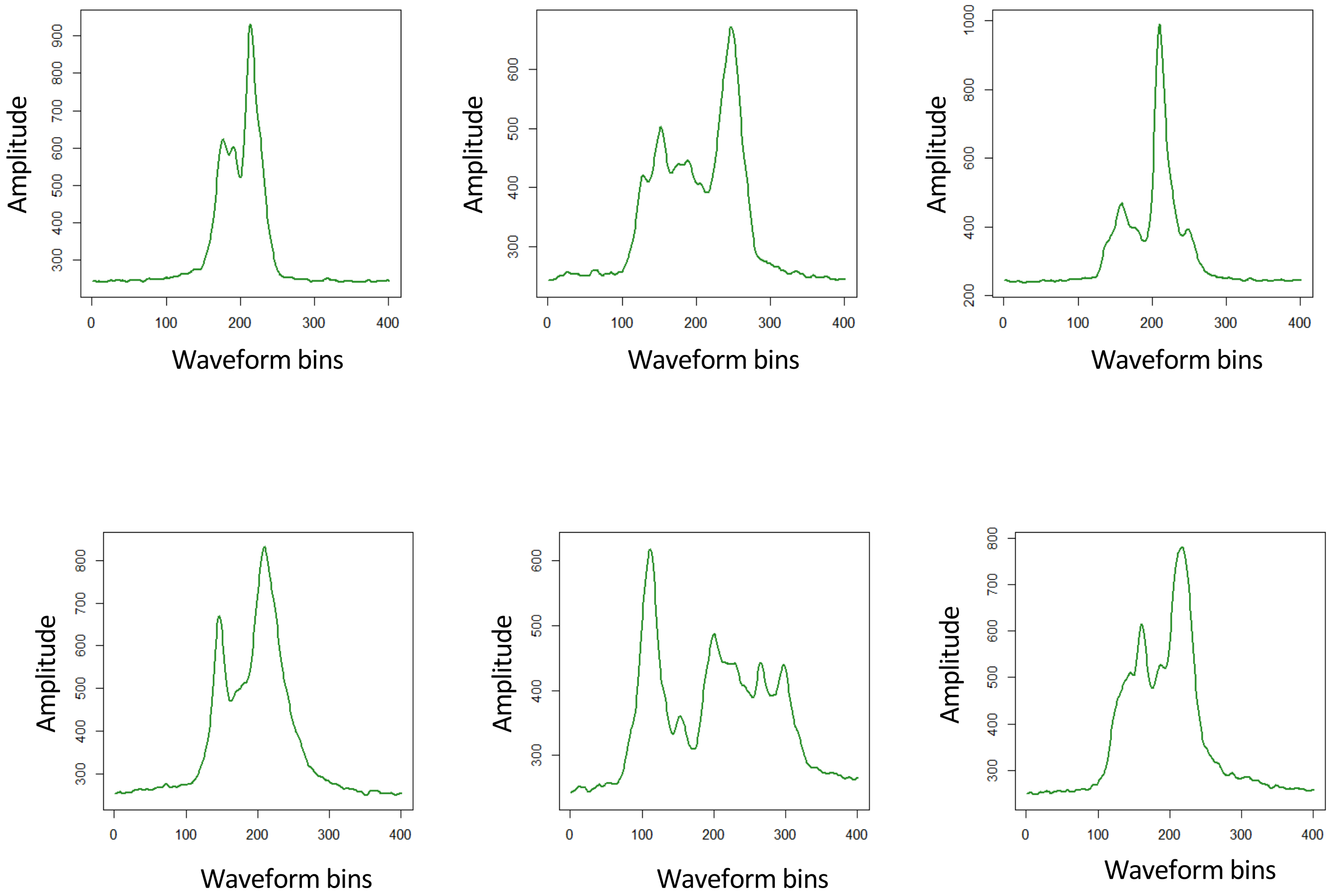

TECIS overlap flightlines and valid waveform

■ Comparison of TECIS and ALS data

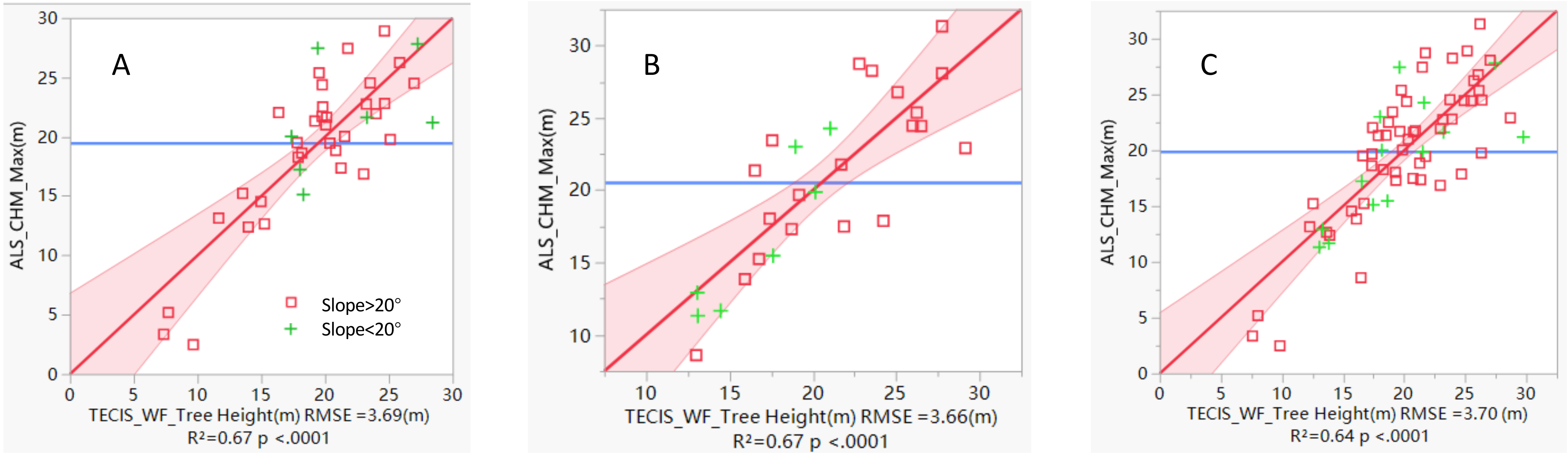

TECIS Waveform(Laser 2) :
SNR>15
Time: 2023.02.06
ALS CHM:
ALS CHM Max<30 m
Metrics : RH_{100}, TE, LE

TECIS Waveform(Laser 4) :
SNR>15
Time: 2023.01.22
ALS CHM:
ALS CHM Max<30 m
Metrics : RH_{100}, TE, LE

TECIS Waveform(A&B) :
SNR>15
Time: 2023.01.22& 02.06
ALS CHM:
ALS CHM Max<30 m
Metrics : RH_{100}, TE, LE

The joint use of Chinese and European satellites

- BRDF reconstruction and validation of multi-angle satellite images (TECIS)

Site:
Pu'er, Yunnan, China.

Date:
20230122.
Local time: 11:57

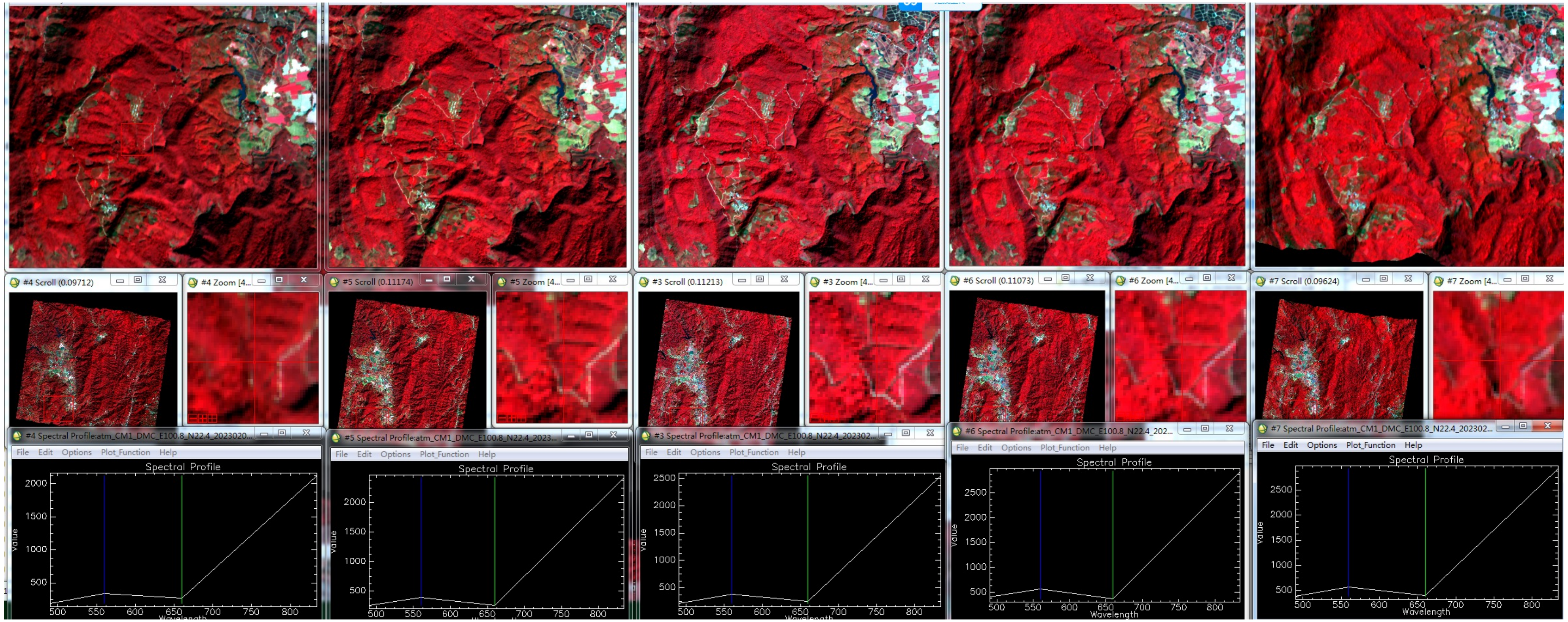

F2M (41°)	F1M (19°)	NAD (0°)	B1M (19°)	B2M (41°)
SZA = 47.4	SZA = 47.3	SZA = 47.3	SZA = 47.2	SZA = 47.2
SAA = 150.2	SAA = 150.3	SAA = 150.4	SAA = 150.6	SAA = 150.8
VZA = 45.0	VZA = 20.5	VZA = 0.4	VZA = 20.5	VZA = 45.1
VAA = 11.2	VAA = 11.4	VAA = 185.0	VAA =191.6	VAA = 191.7

Reconstructed images

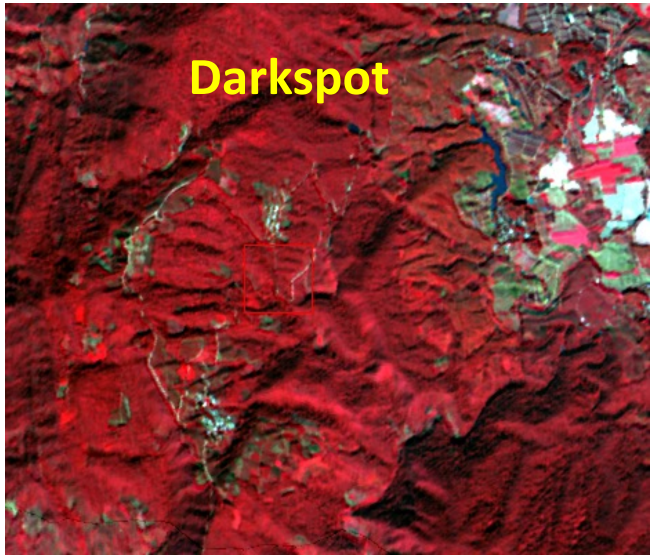

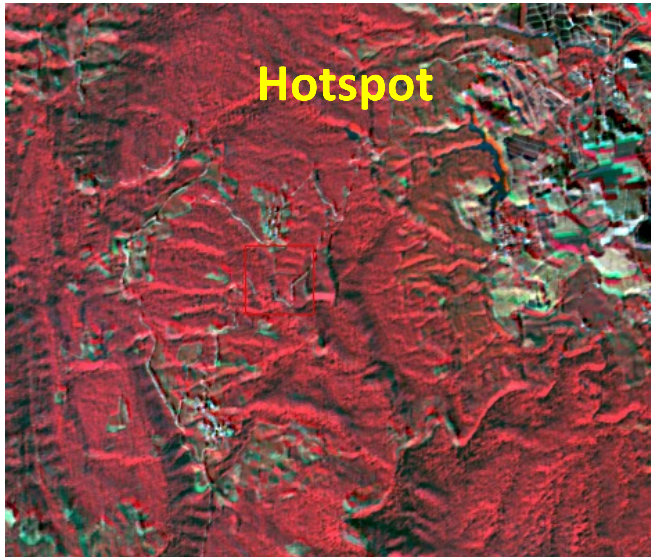

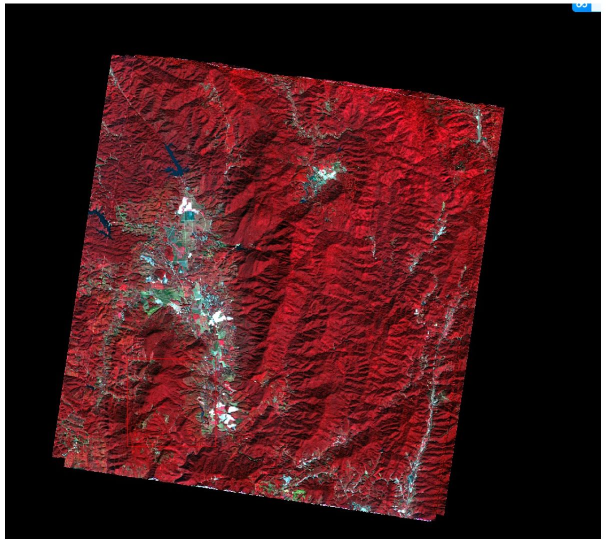

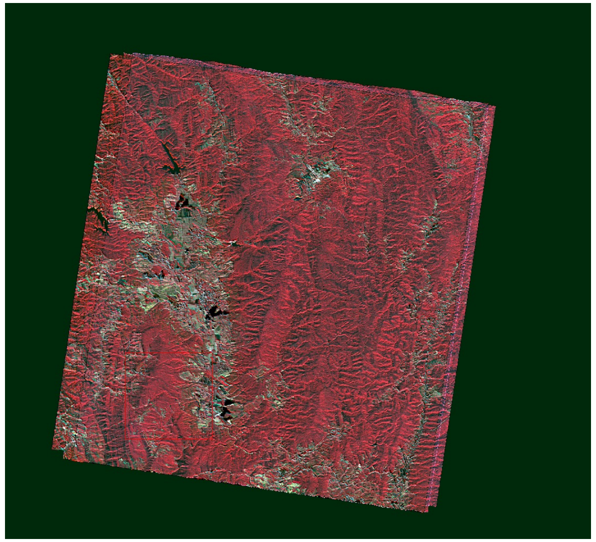

The joint use of Chinese and European satellites

Site:
Pu'er, Yunnan province,China.

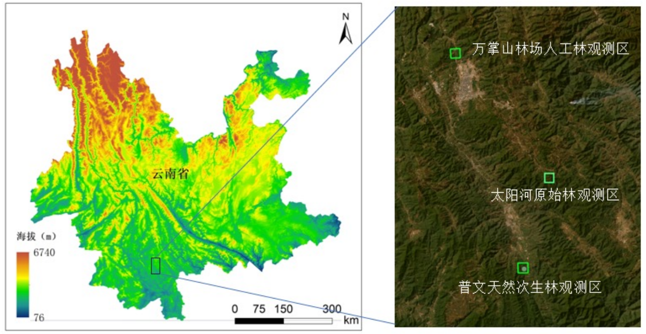

•GF-6：2020-12-14 12:26
SZA = 47.0°, SAA = 164.9°
Blue Band (B1): 0.45μm to 0.52μm
Green Band (B2): 0.52μm to 0.60μm
Red Band (B3): 0.63μm to 0.69μm
NIR Band (B4): 0.76μm to 0.90μm
Spatial Resolution: 16 meters

•Airborne HSI：2020-12-13 13:47
SZA = 47.6°, SAA = 196.2°
Spectral Range: **0.40μm~0.96μm**
Spectral Resolution: 4.8 nm
Resample the airborne imagery's spatial resolution from 1 meter to match that of the GF-6 imagery, which is 16 meters.

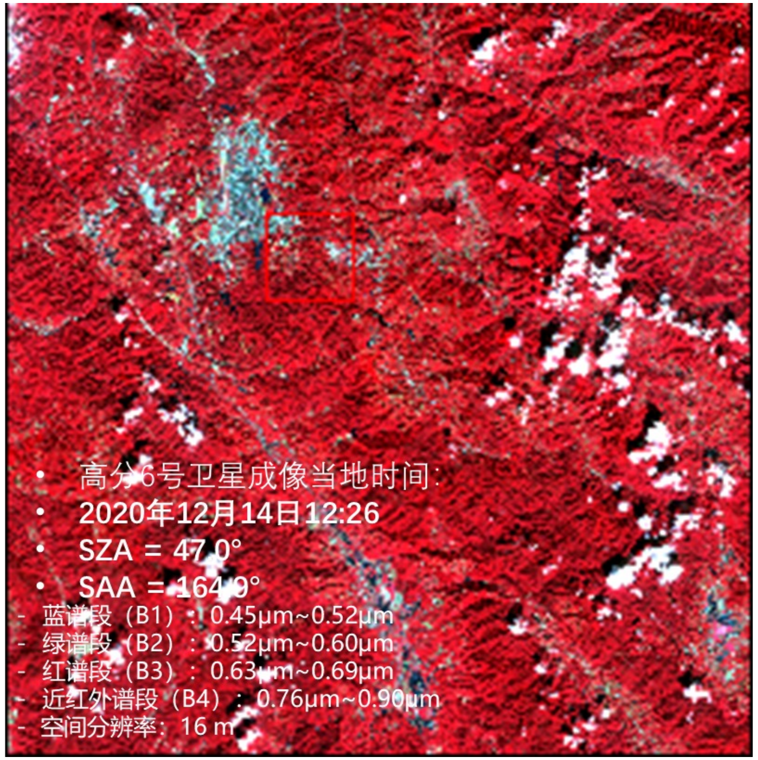

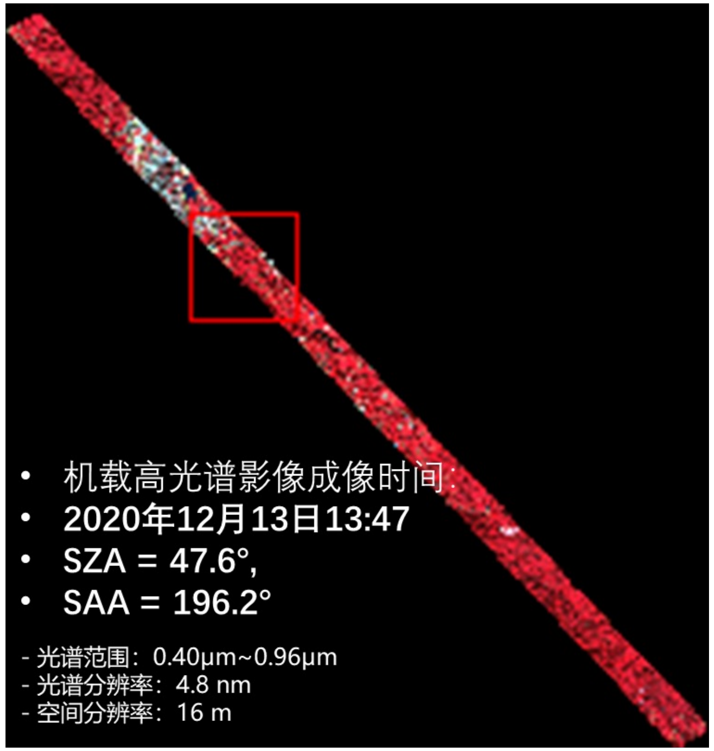

Poster ID：278

P.6.2: ECOSYSTEMS

Time:
Tuesday, 12/Sept/2023:
4:09pm – 4:17pm

Room:
312 - Continuing Education College (CEC)

Authors: Wen Jia, Yong Pang*

Poster Title: Satellite Reflectance Validation based on BRDF Reconstructed Airborne Hyperspectral Data.

Monitoring forest stand dynamics after windthrow

2006 2011 2016 2021

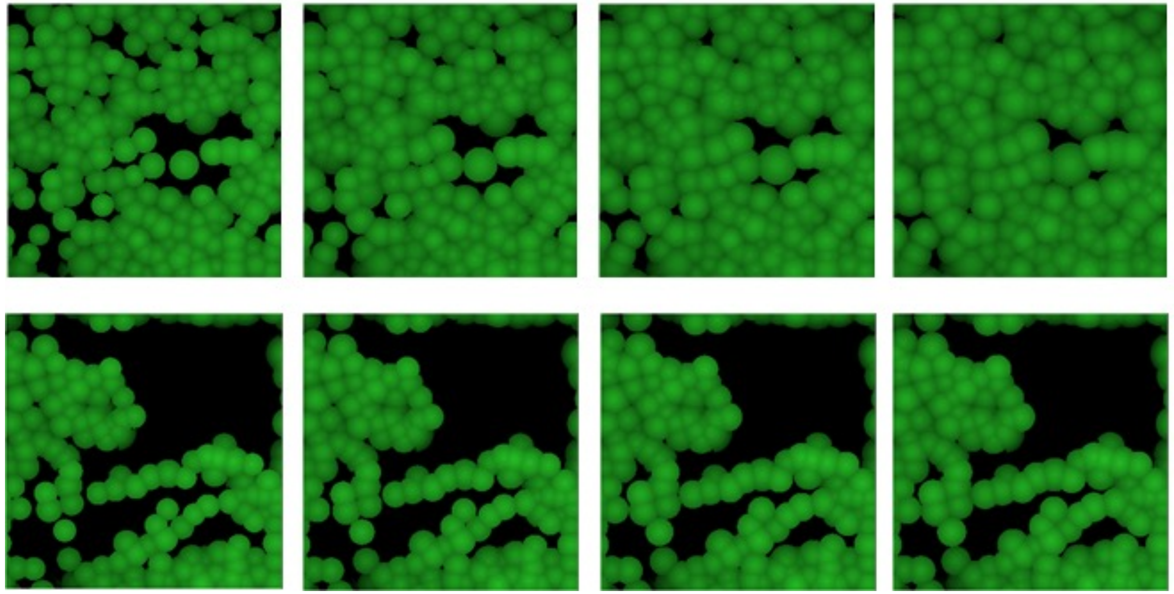

LiDAR in 2021

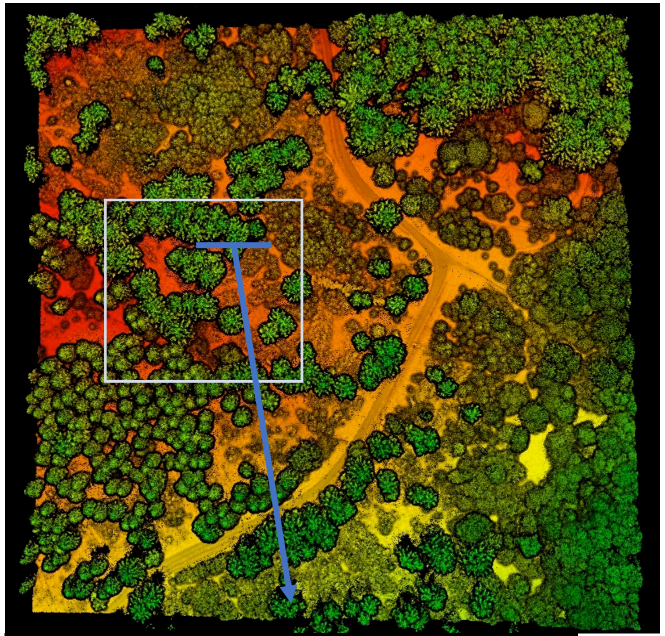

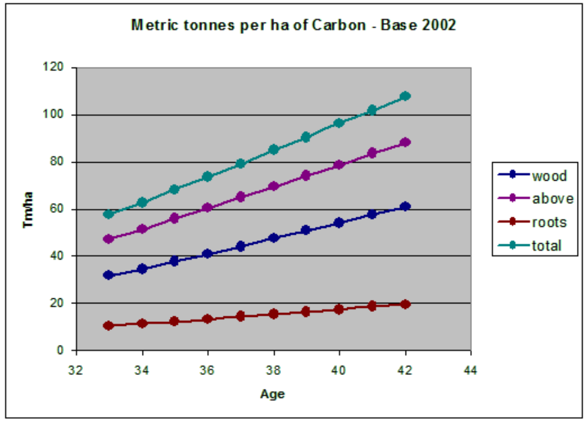

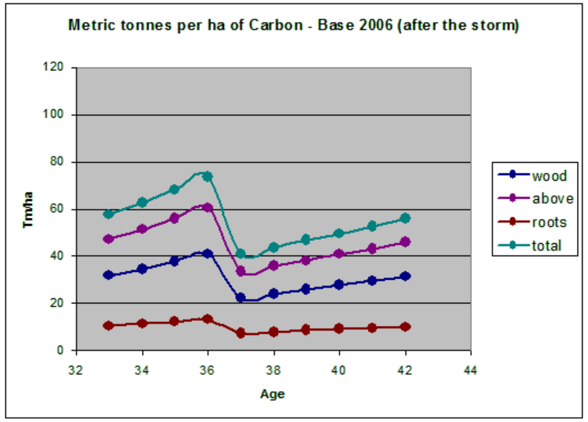

LiDAR and TASS simulations

Background

Sitka spruce is the main forestry plantation species across Great Britain accounting for more than a third of all forest estate[1]

Increasing drought due to climate change will decrease productivity. Reducing carbon sequestration[2] and yields and increasing mortality[3]

Monitoring and detecting early drought stress can inform us of current forest health. Selecting more drought tolerant strains can improve future forest resilience

Aims

- Expose breeding population S. spruce clones to drought
- Identify vegetation indices sensitive to drought stress
- Compare drought tolerance of clones

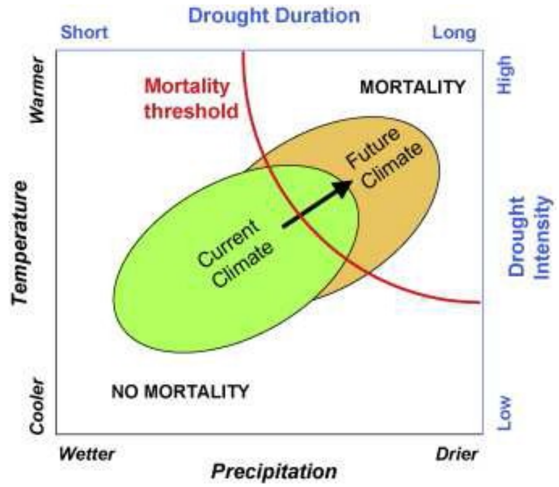

Climate change scenarios

Climatic suitability – Sitka spruce http://www.forestdss.org.uk/geoforestdss/esc4.jsp

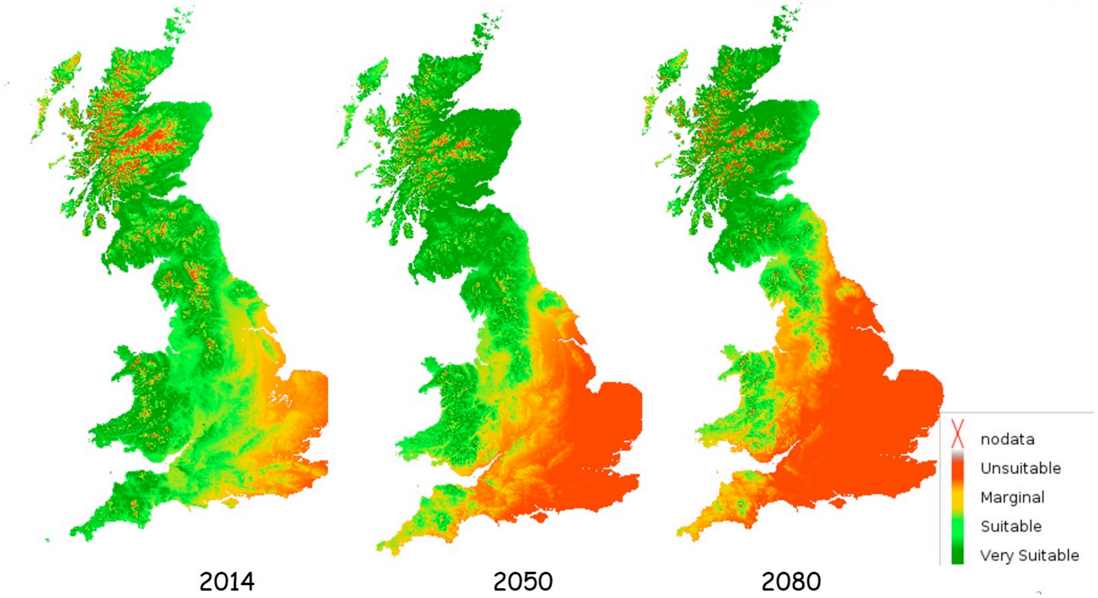

Vegetation Indices (VI)

NDVI – Normalised difference Vegetation Index
Sensitive to **Chlorophyll content** or 'Greenness"

ARI – Anthocyanin Reflectance Index
Sensitive to **Anthocyanins** (light screening)

PRI – Photochemical Reflectance Index
Sensitive to **Carotenoids** (energy dissipation)

NDWI – Normalised Difference Water Index
Sensitive to **needle water content**

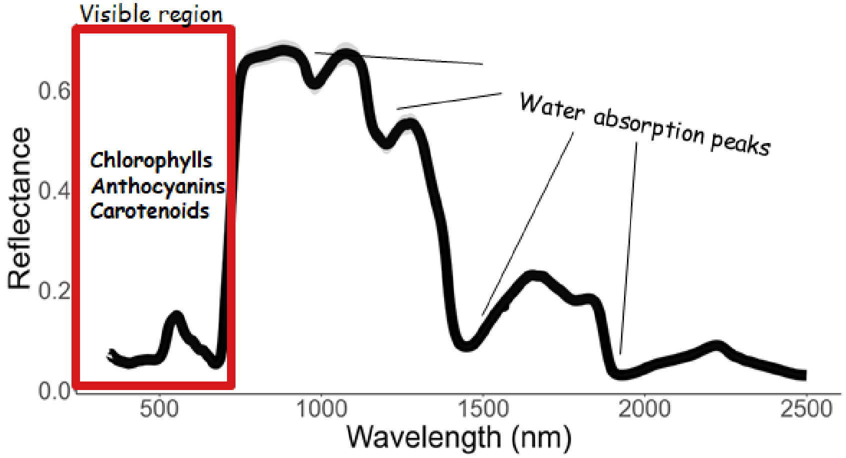

VIs	Equation	Reference
NDVI	(NIR – Red)/(NIR + Red)	Rouse *et al*. (1974)
NDVI-RE	(NIR – Red-edge)/(NIR + Red-edge)	Gitelson and Merzlyak (1994)
GRVI	(Green – Red)/(Green + Red)	Tucker (1979)
GNDVI	(NIR – Green)/(NIR + Green)	Gitelson *et al*. (1996)
MTCI	(NIR - Red-edge)*(Red-edge - Red)	Dash and Curran (2004)
ARI	$(1/R_{550}) - (1/R_{700})$	Gitelson *et al*. (2001)

Abbreviations: ARI = Anthocyanin Reflectance Index; GNDVI = Green Normalised Difference Vegetation Index; GRVI = Green Red Vegetation Index; MTCI = MERIS Terrestrial Chlorophyll Index;

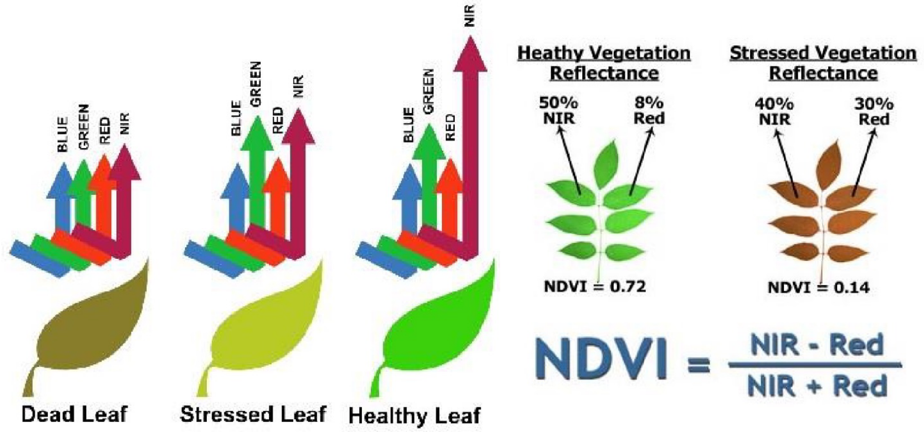

Polytunnel experiments

Polytunnel experiment

- Drought and Control groups
- 6 clones
- 8-week drought period
- Weekly reflectance measurements

Drought stress in Sitka spruce in polytunnel experiments

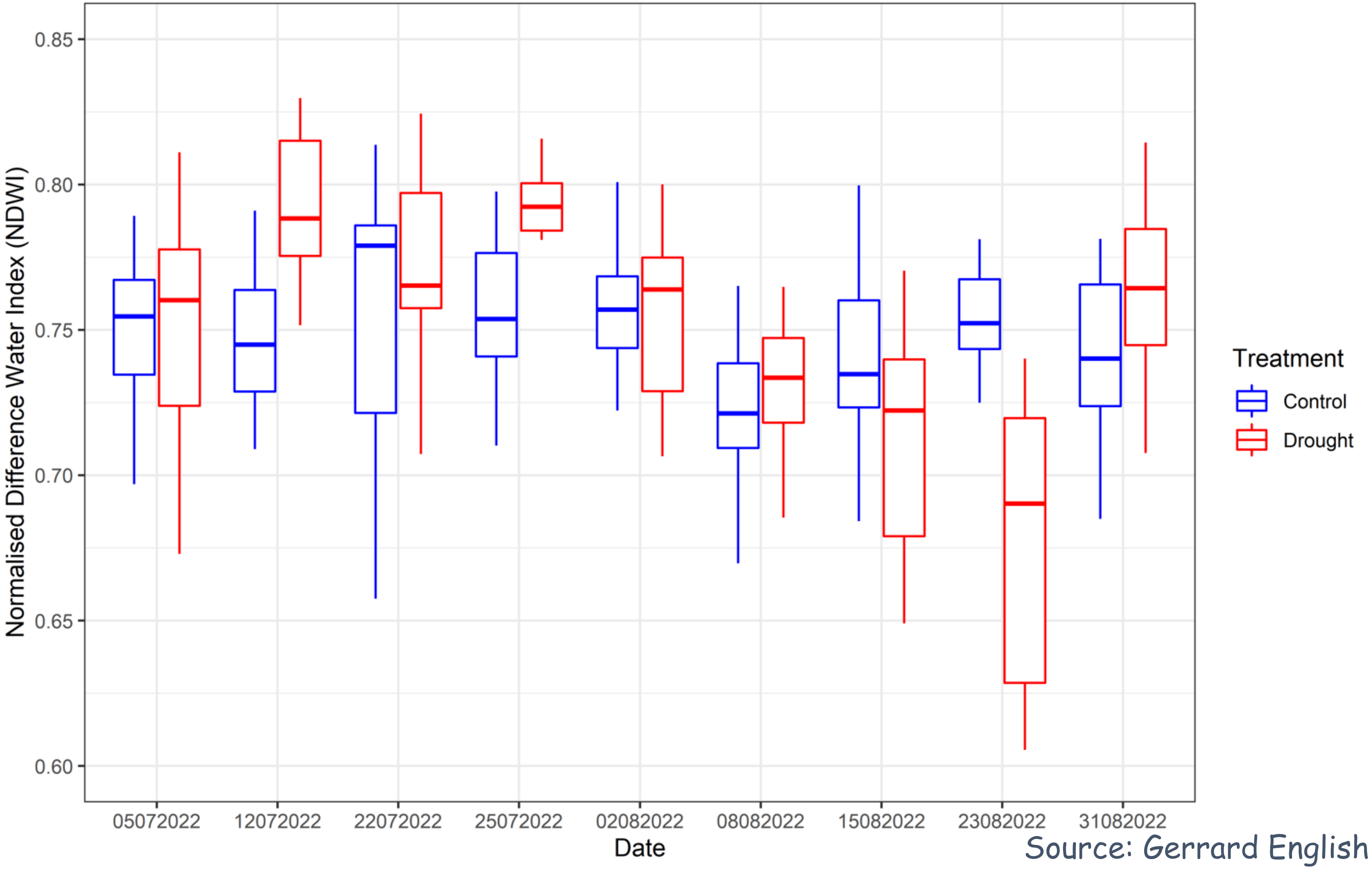

Source: Gerrard English PhD

Drought stress in Sitka spruce in polytunnel experiments

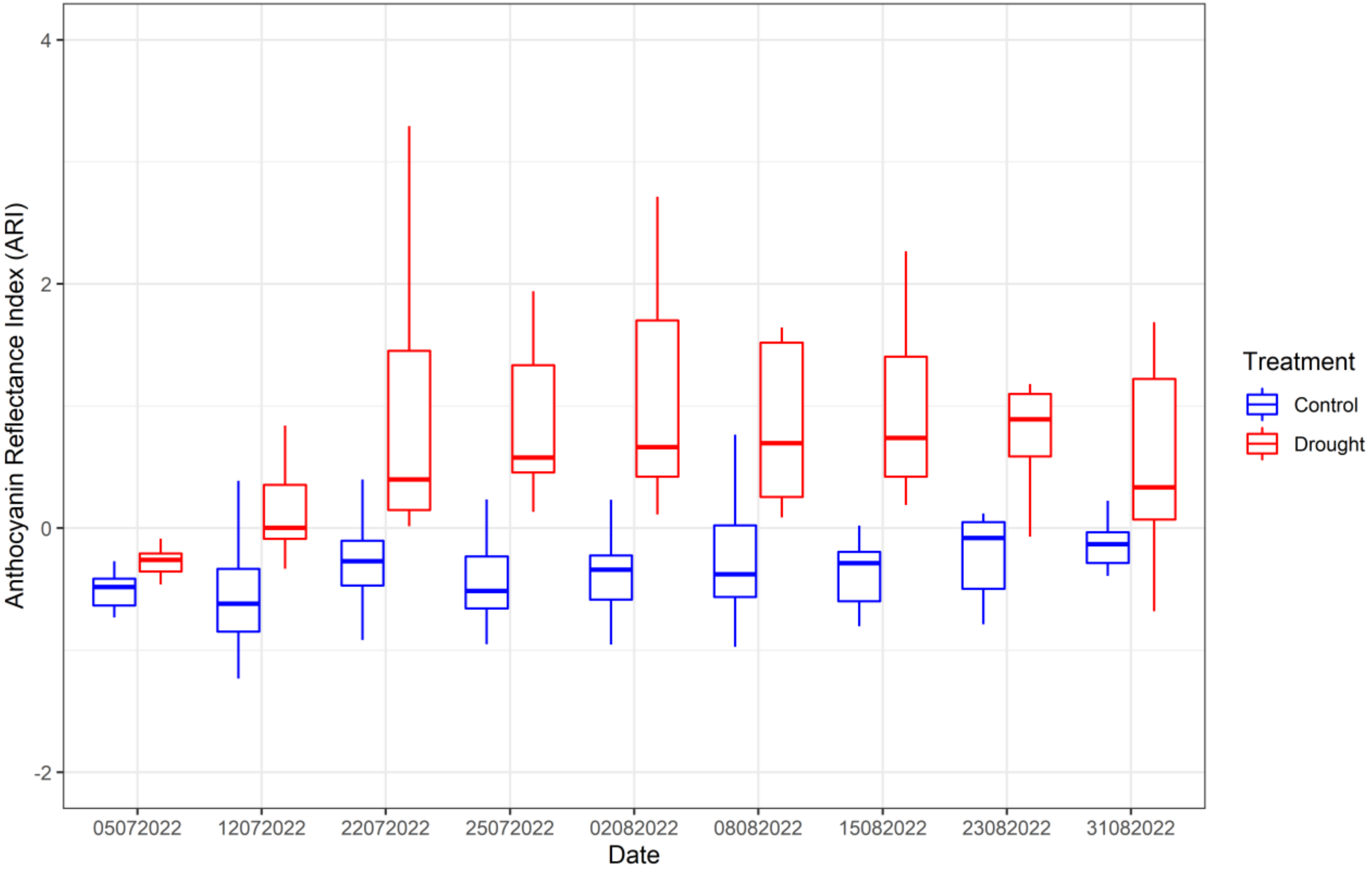

Source: Gerrard English PhD

Drought stress in Sitka spruce in polytunnel experiments

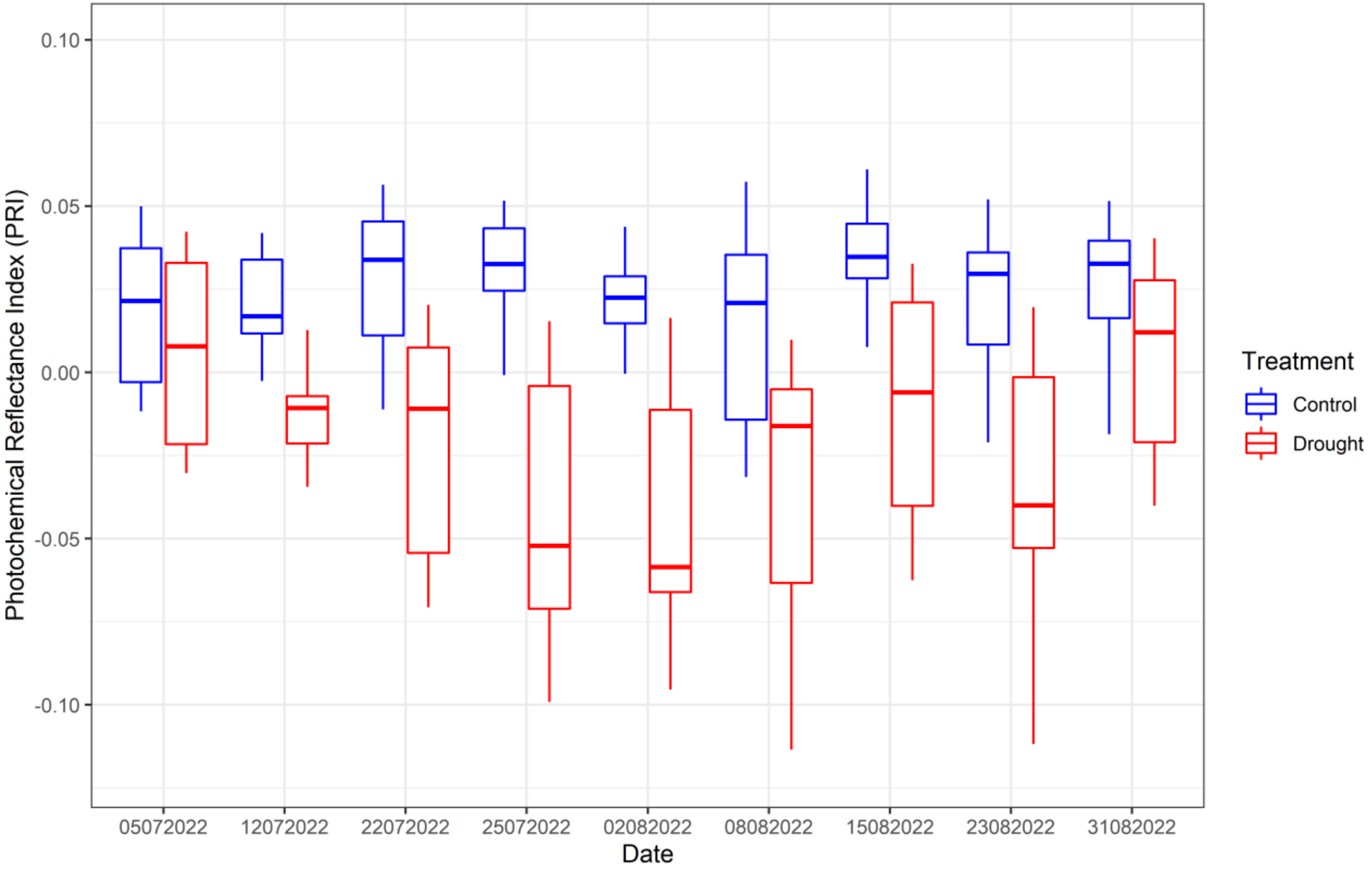

Source: Gerrard English PhD

Mapping trajectories of stress

Paramount to early detection is the understanding of the processes of infection and the response mechanisms of different phenotypes

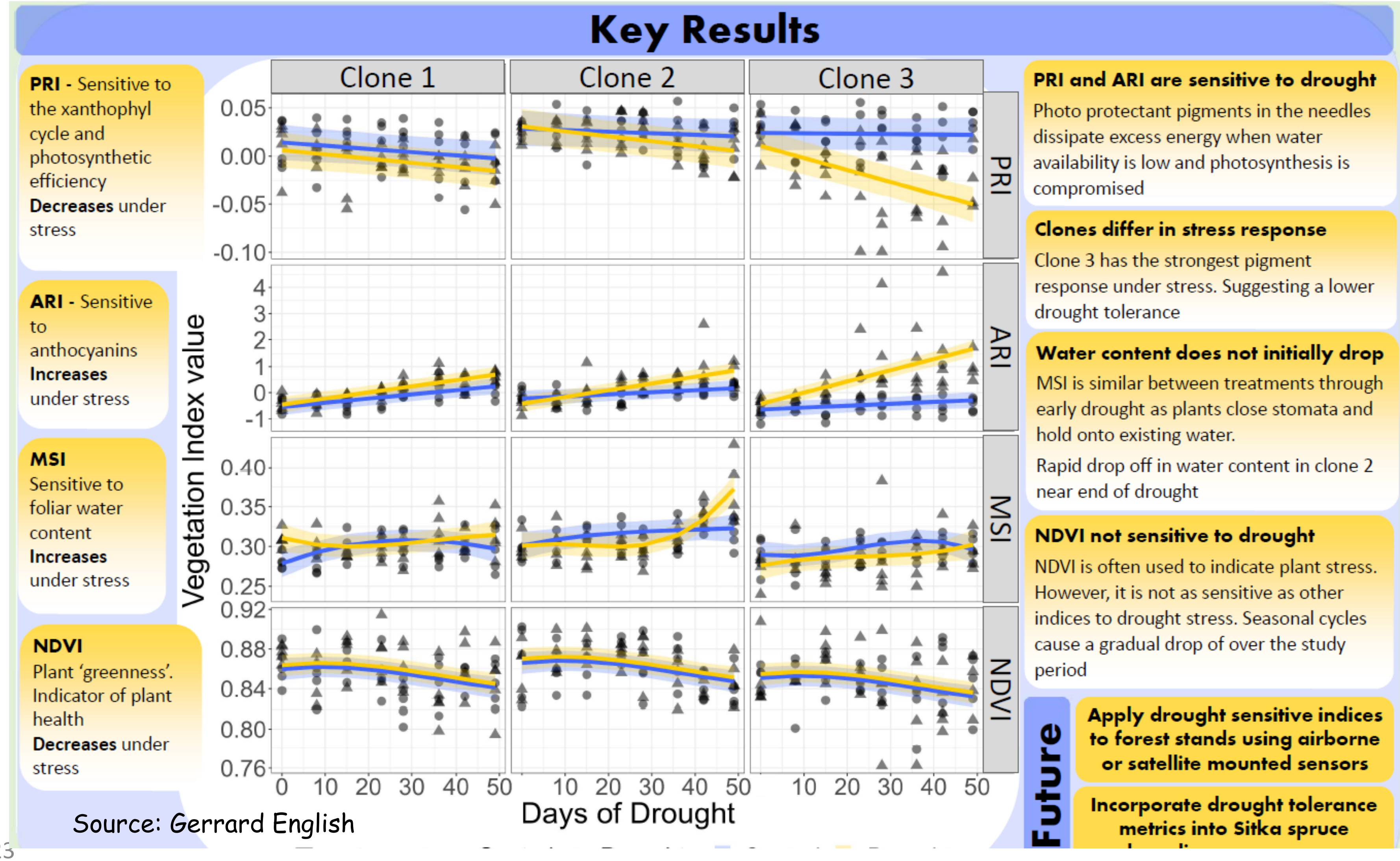

Source: Gerrard English

Monitoring processes with Time-series of satellite imagery in GEE

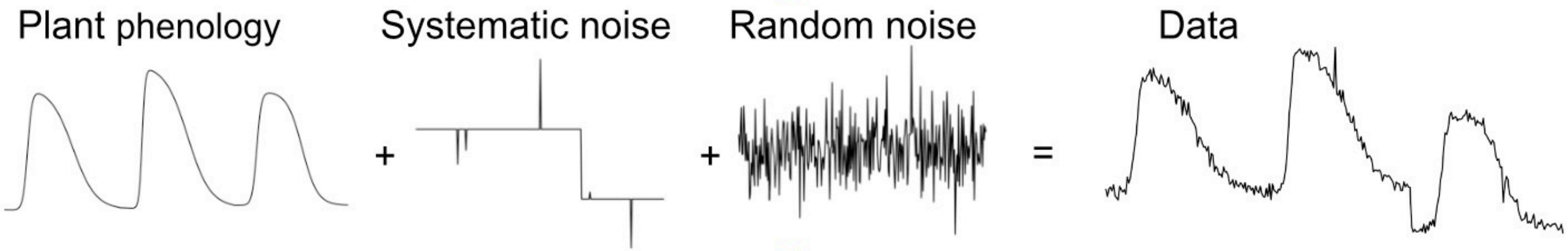

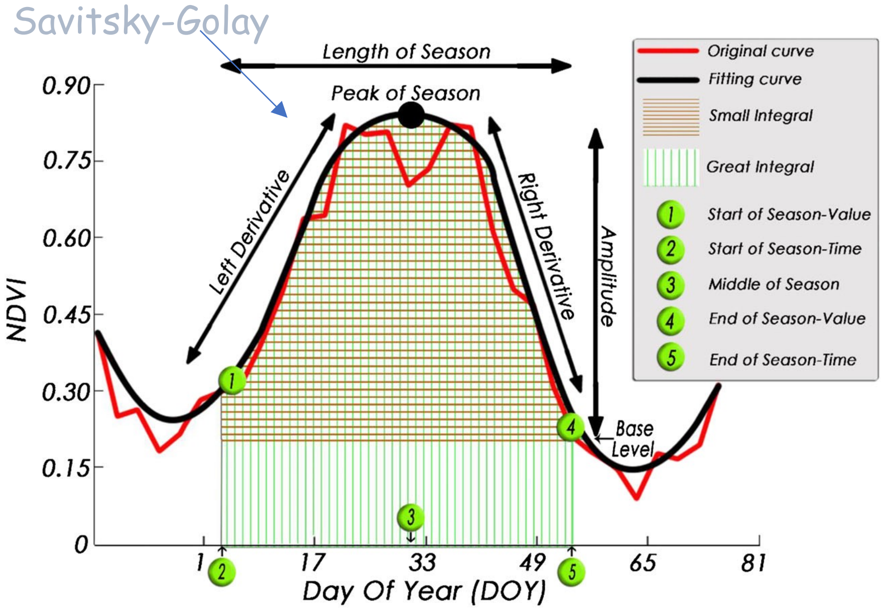

All seasonal parameters can be extracted using the TIMESAT algorithm (Lebrini et al., 2020)

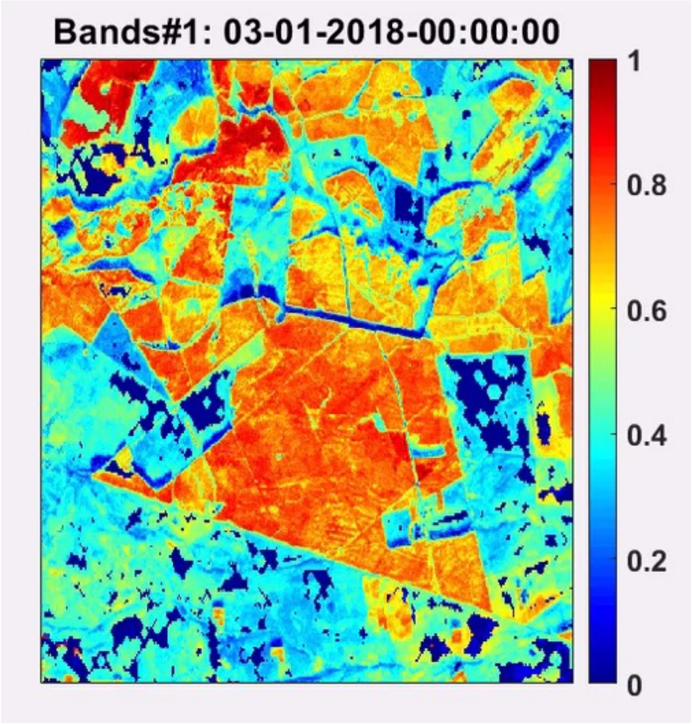

Harwood forest in Kielder F.D.

Weighted Principal Component Analysis (WPCA).

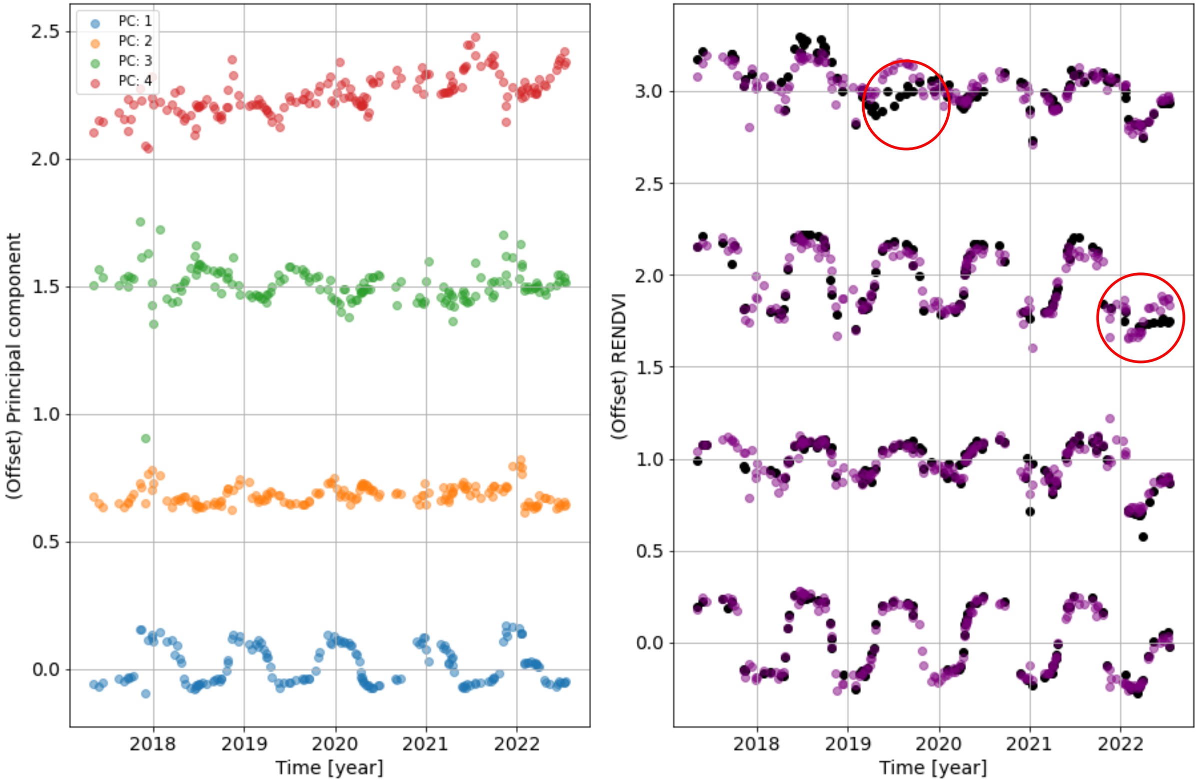

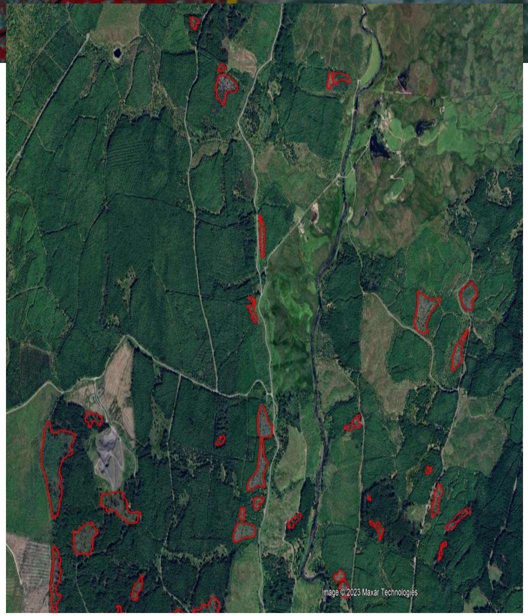

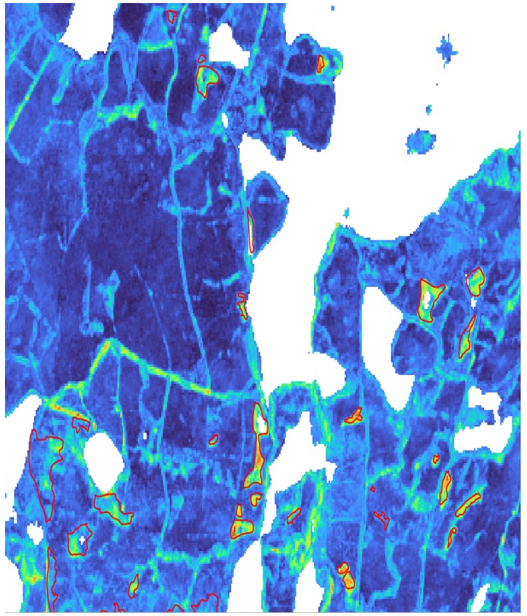

Anomalies are flagged for pixel time series where the observations deviate from the WPCA model predictions. These can highlight felling, or diseases affecting the canopy of trees etc. Conversely, observations for healthy vegetation should show good agreement between the model and data.

Clouds are a problem

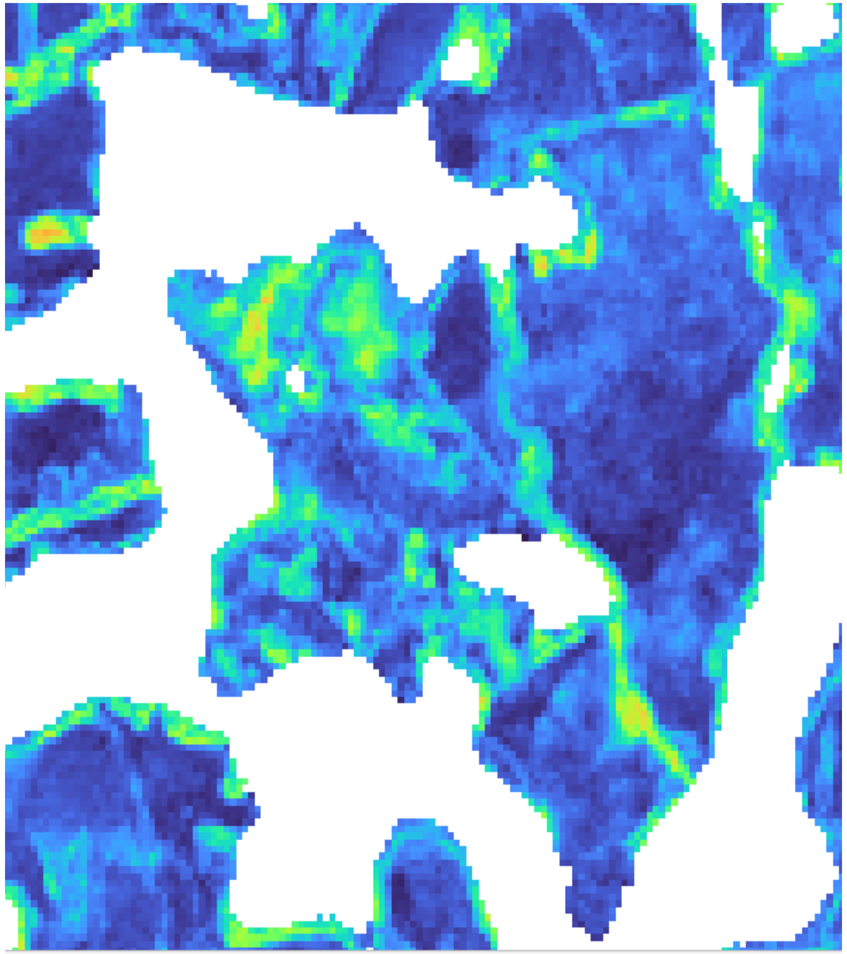

Co-aligned Hyperspectral and LiDAR
Headwall systems

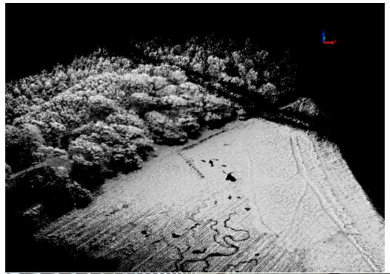

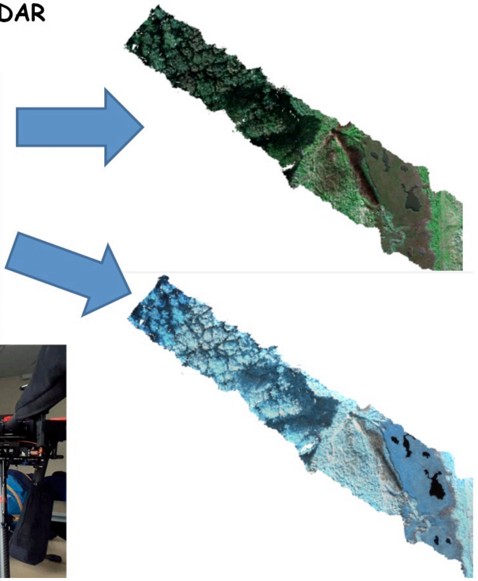

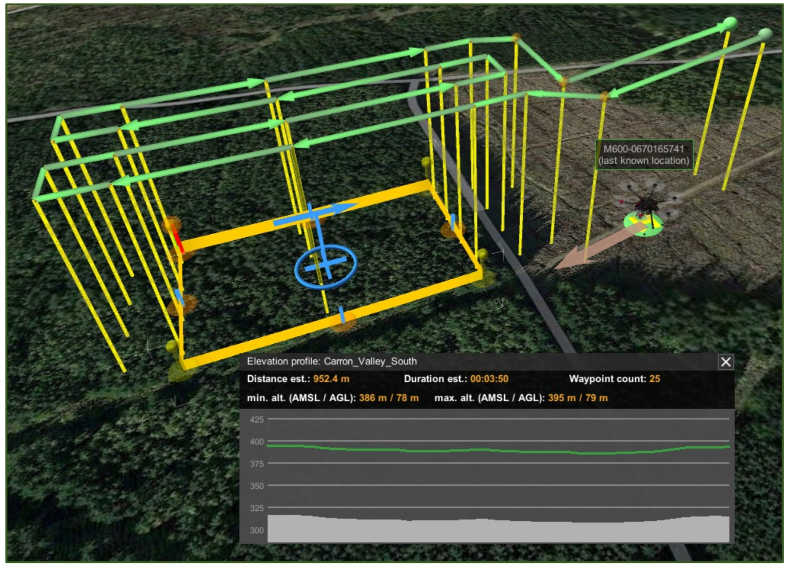

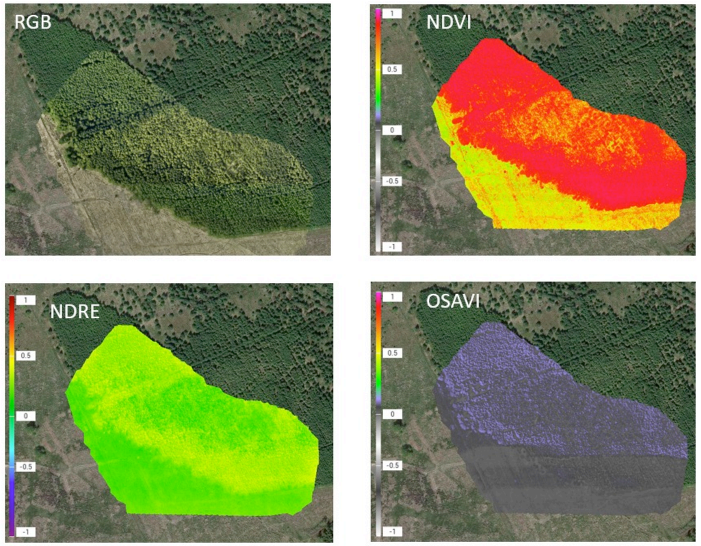

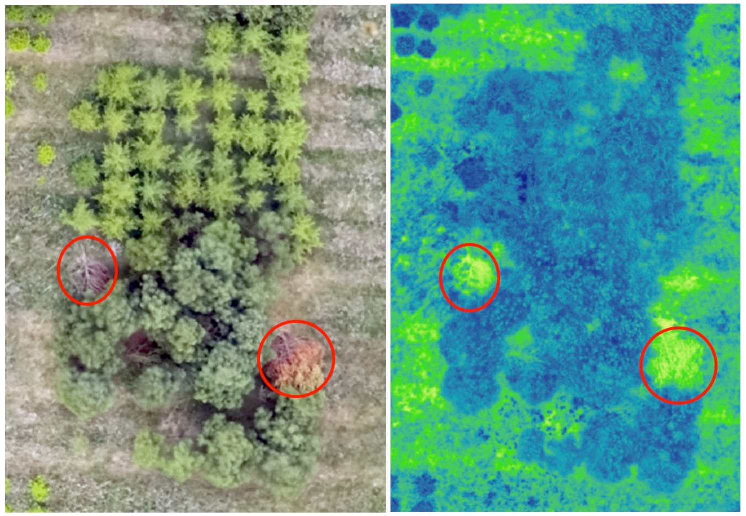

PolyPens

- Field spectroradiometer
- Collect hundreds of samples
- GPS referenced
- Can be operated by non-expert
- It can be customised to calculate VIs

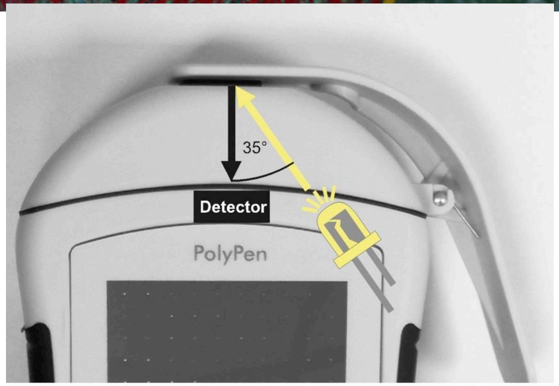

Samples are introduced in a small probe window that it is illuminated by a full-spectrum light

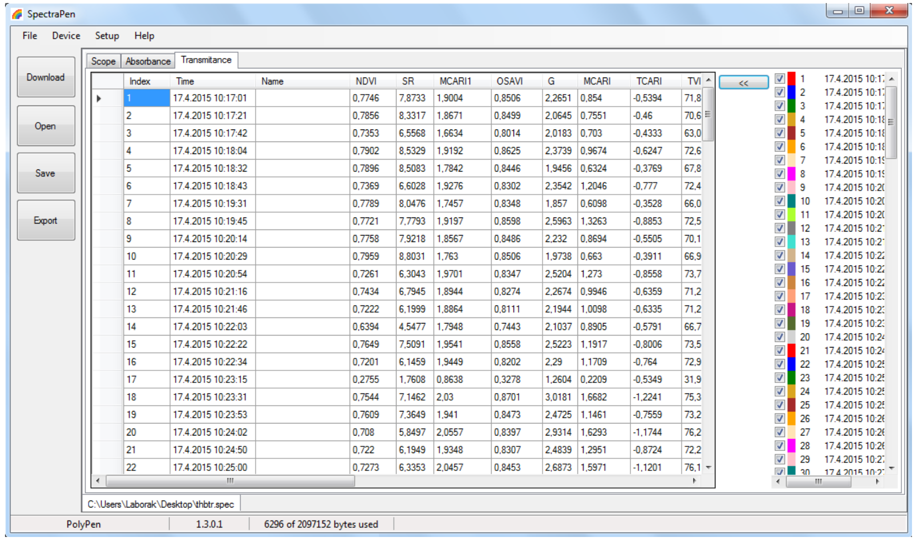

Index	Time	Name	NDVI	SR	MCARI1	OSAVI	G	MCARI	TCARI	TVI
1	17.4.2015 10:17:01		0,7746	7,8733	1,9004	0,8506	2,2651	0,854	-0,5394	71,8
2	17.4.2015 10:17:21		0,7856	8,3317	1,8671	0,8499	2,0645	0,7551	-0,46	70,6
3	17.4.2015 10:17:42		0,7353	6,5568	1,6634	0,8014	2,0183	0,703	-0,4333	63,0
4	17.4.2015 10:18:04		0,7902	8,5329	1,9192	0,8625	2,3739	0,9674	-0,6247	72,6
5	17.4.2015 10:18:32		0,7896	8,5083	1,7842	0,8446	1,9456	0,6324	-0,3769	67,8
6	17.4.2015 10:18:43		0,7369	6,6028	1,9276	0,8302	2,3542	1,2046	-0,777	72,4
7	17.4.2015 10:19:31		0,7789	8,0476	1,7457	0,8348	1,857	0,6098	-0,3528	66,0
8	17.4.2015 10:19:45		0,7721	7,7793	1,9197	0,8598	2,5963	1,3263	-0,8853	72,5
9	17.4.2015 10:20:14		0,7758	7,9218	1,8567	0,8486	2,232	0,8694	-0,5505	70,1
10	17.4.2015 10:20:29		0,7959	8,8031	1,763	0,8506	1,9738	0,663	-0,3911	66,9
11	17.4.2015 10:20:54		0,7261	6,3043	1,9701	0,8347	2,5204	1,273	-0,8558	73,7
12	17.4.2015 10:21:16		0,7434	6,7945	1,8944	0,8274	2,2674	0,9946	-0,6359	71,2
13	17.4.2015 10:21:46		0,7222	6,1999	1,8864	0,8111	2,1944	1,0098	-0,6335	71,2
14	17.4.2015 10:22:03		0,6394	4,5477	1,7948	0,7443	2,1037	0,8905	-0,5791	66,7
15	17.4.2015 10:22:22		0,7649	7,5091	1,9541	0,8558	2,5223	1,1917	-0,8006	73,5
16	17.4.2015 10:22:34		0,7201	6,1459	1,9449	0,8202	2,29	1,1709	-0,764	72,9
17	17.4.2015 10:23:15		0,2755	1,7608	0,8638	0,3278	1,2604	0,2209	-0,5349	31,9
18	17.4.2015 10:23:31		0,7544	7,1462	2,03	0,8701	3,0181	1,6682	-1,2241	75,3
19	17.4.2015 10:23:53		0,7609	7,3649	1,941	0,8473	2,4725	1,1461	-0,7559	73,2
20	17.4.2015 10:24:02		0,708	5,8497	2,0557	0,8397	2,9314	1,6293	-1,1744	76,2
21	17.4.2015 10:24:50		0,722	6,1949	1,9348	0,8307	2,4839	1,2951	-0,8724	72,2
22	17.4.2015 10:25:00		0,7273	6,3353	2,0457	0,8453	2,6873	1,5971	-1,1201	76,1

More intensive Forest Inventories

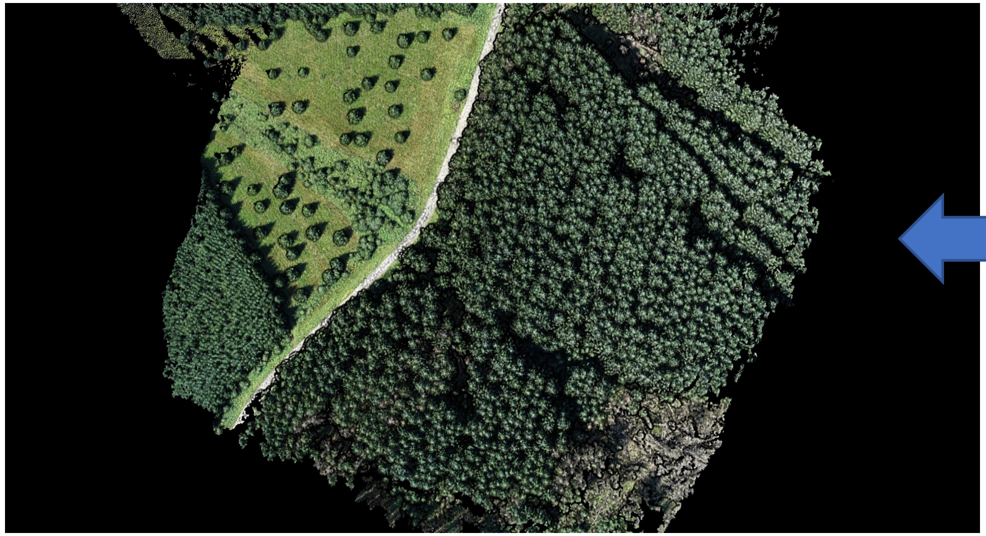

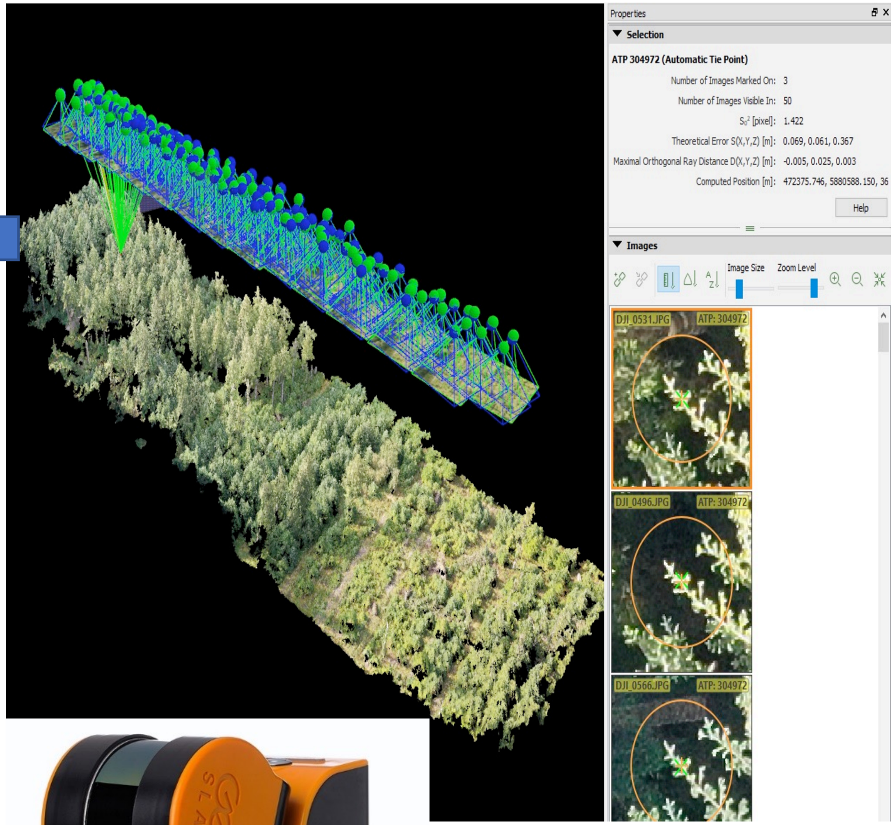

Structure from Motion (SfM)

More intensive Forest Inventories

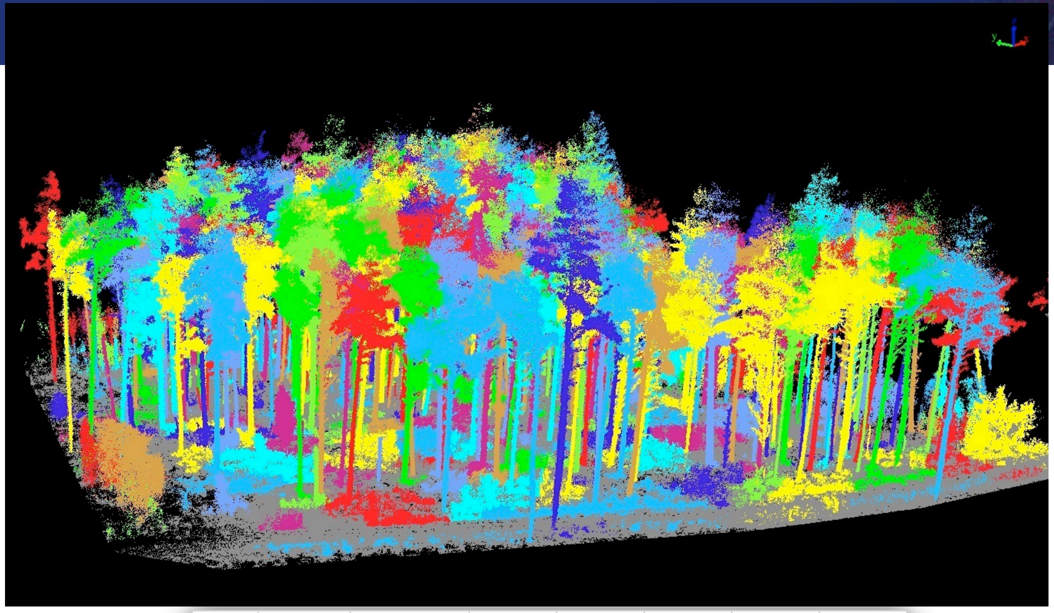

TreeID	Tree LocationX	Tree LocationY	Tree Height	DBH	Crown Diameter	Crown Area	Crown Volume
1	241136.5	708116.752	22.683	0.108	6.158	29.787	171.204
2	241156.6	708130.169	16.734	0.141	2.807	6.189	23.876
3	241156.6	708114.448	20.412	0.315	4.182	13.738	63.35
4	241144.5	708118.63	20.983	0.283	4.684	17.23	103.962
5	241145	708129.461	17.014	0.233	4.981	19.486	66.312
6	241153.9	708130.09	17.943	0.275	3.867	11.742	61.339
7	241139.7	708117.187	2.516	0	0.837	0.55	0.779
8	241151.3	708126.85	17.599	0.269	4.815	18.21	87.958
9	241154.7	708113.868	5.206	0.085	2.328	4.258	5.464
10	241142.6	708109.197	2.785	0.908	0.483	0.184	0.142
11	241156.4	708127.288	4.584	0.127	0.454	0.162	0.492
12	241147.3	708121.923	17.541	0.309	5.152	20.847	114.277
13	241129	708120.23	2.18	0.42	0.859	0.58	0.708
14	241139.3	708130.346	17.071	0.203	4.423	15.367	57.879
15	241143.8	708117.128	2.196	0.325	2.191	3.769	3.87
16	241140	708128.533	17.83	0.273	3.776	11.2	64.24
17	241130.8	708120.931	17.424	0.578	6.754	35.823	161.829
18	241126.6	708124.623	3.986	0.373	0.655	0.337	0.487
19	241150.2	708120.727	17.765	0.263	4.931	19.095	98.912

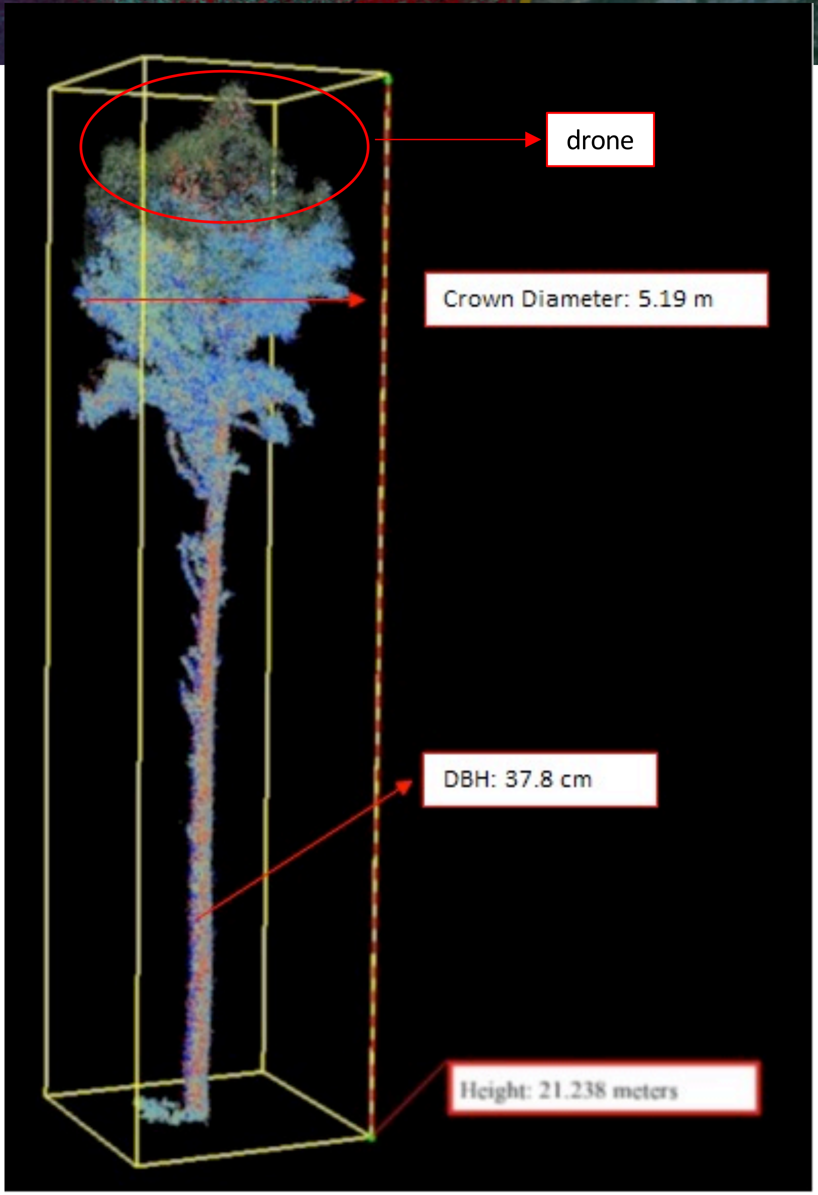

Reconstruction of stem profiles

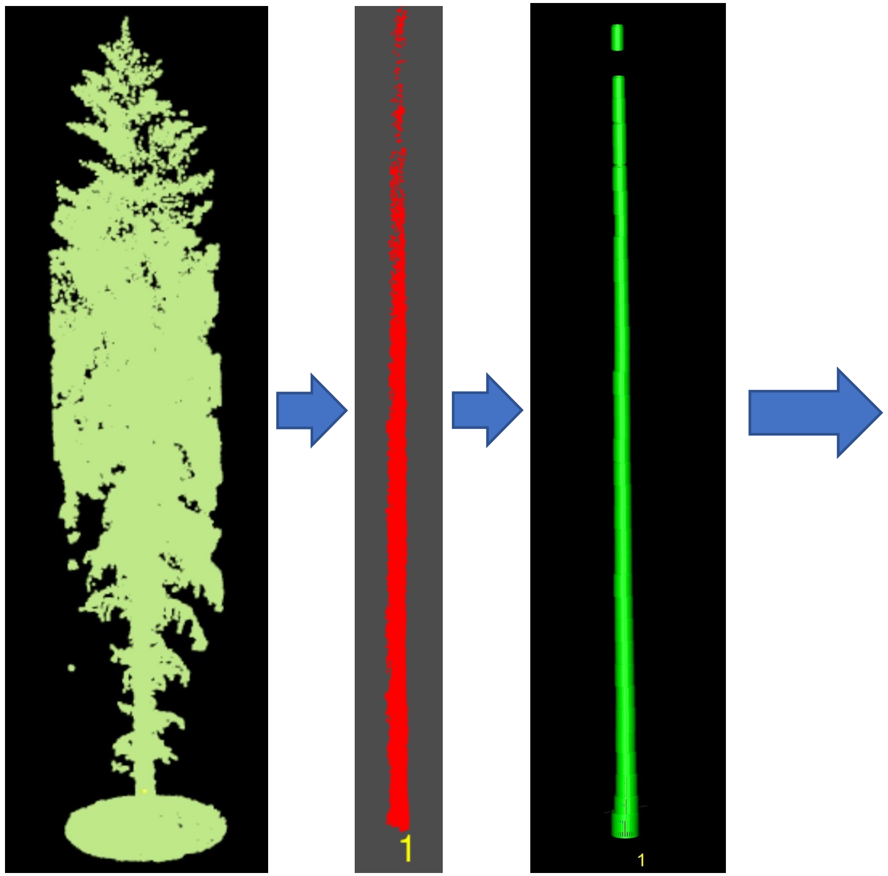

	TreeID	Segment	X	Y	Radius	Error	AvgHeight	N
1	1	1	-17.53903	7.037840	0.29234796	0.0014862970	0.3656768	1084
2	1	2	-17.56081	7.025208	0.25654544	0.0007262826	0.7480973	2598
3	1	3	-17.57246	7.033874	0.23164961	0.0007324386	1.2470507	2187
4	1	4	-17.59054	7.043299	0.21158950	0.0006658642	1.7538767	2279
5	1	5	-17.59245	7.062224	0.20760750	0.0006143630	2.2538120	2349
6	1	6	-17.59744	7.061986	0.20681464	0.0007376114	2.7449919	1980
7	1	7	-17.60485	7.075518	0.20374520	0.0008178060	3.2450518	1911
8	1	8	-17.60522	7.087647	0.20018794	0.0006331408	3.7421126	1806
9	1	9	-17.60551	7.097774	0.19801973	0.0006362345	4.2541146	1592
10	1	10	-17.60834	7.101378	0.19314777	0.0007074113	4.7416008	1620
11	1	11	-17.60534	7.111123	0.19282668	0.0007393210	5.2472676	1739
12	1	12	-17.59714	7.115566	0.19008622	0.0009818980	5.7443693	1301
13	1	13	-17.59986	7.115121	0.17958328	0.0008372263	6.2580303	1273
14	1	14	-17.59743	7.119706	0.18212190	0.0009800801	6.7533206	1263
15	1	15	-17.60035	7.123136	0.18225153	0.0011998649	7.2562225	1098
16	1	16	-17.60144	7.124760	0.17653747	0.0011435685	7.7432031	1112
17	1	17	-17.60380	7.137519	0.18135210	0.0012792960	8.2274332	962
18	1	18	-17.60251	7.152461	0.18171898	0.0013329007	8.7584915	968
19	1	19	-17.60418	7.132808	0.16686686	0.0015148452	9.2613016	817
20	1	20	-17.60565	7.136744	0.16927358	0.0022116890	9.7254893	606
21	1	21	-17.60639	7.161991	0.17636872	0.0013957290	10.2471290	731
22	1	22	-17.60936	7.137662	0.15913918	0.0017389435	10.7609714	573
23	1	23	-17.62312	7.140086	0.15708909	0.0024288684	11.2370986	436
24	1	24	-17.61830	7.152087	0.15605877	0.0023002041	11.7480889	378
25	1	25	-17.61791	7.151719	0.14960401	0.0024284949	12.2424251	371
26	1	26	-17.61489	7.160408	0.15124548	0.0030171064	12.7291011	275
27	1	27	-17.61248	7.165521	0.14717513	0.0031003842	13.2232044	270
28	1	28	-17.61167	7.153258	0.13773561	0.0041274031	13.7534276	174
29	1	29	-17.60246	7.165888	0.14434142	0.0045682638	14.2172584	113
30	1	30	-17.59347	7.178635	0.14867545	0.0052401965	14.7412882	102

Source: Jaz Stoddart

Report on the peer reviewed publications after 3 years of activity

1. Liming Du, Yong Pang*, Wenjian Ni, Xiaojun Liang, Zengyuan Li, Juan Suárez & Wei Wei. (2023). Forest terrain and canopy height estimation using stereo images and spaceborne LiDAR data from GF-7 satellite. Geo-spatial Information Science. Dragon Programme Special Issue.
2. Li He, Yong Pang*, Zhongjun Zhang, Xiaojun Liang, & Bowei Chen. (2023). ICESat-2 Data Classification and Estimation of Terrain Height and Canopy Height. International Journal of Applied Earth Observation and Geoinformation. 118, 103233, 1-14.
3. Shili Meng, Yong Pang*, Kebiao Huang & Zengyuan Li. (2023). A patch filling method for thematic map refinement: a ca se study on forest cover mapping in the Greater Mekong Subregion and Malaysia. GIScience & Remote Sensing, 60(1)-2252225: 1-21.
4. Shili Meng, Yong Pang*, Chengquan Huang, & Zhen Li. (2022). Improved forest cover mapping by harmonizing multiple land cover products over China. *GIScience & Remote Sensing*, *59*(1), 1570-1597.
5. Ming Yan, Yong Pang*, Yunling He, Shili Meng & Wei Wei (2023). Land Cover Mapping of Pu'er City Based on GEE Cloud Platform and Sentinel-2 Data. Remote Sensing Technology and Application, 38(2): 432-442.
6. Ming Yan, Yong Pang*, Yunling He & Shili Meng (2023). Consistency Analysis and Accuracy Evaluation of Multi-Source Land Cover Products in Pu'er. Forest Resources Management,173-182.
7. Luxia Liu, Yong Pang*, Guoqing Sang, Zengyuan Li, & Bo Hu. (2022). High resolution remote sensing estimation of tree species diversity in the Pu'er monsoon evergreen broad-leaved forest. Acta Ecologica Sinica,42(20):8398-8413.
8. Zhiyong Qi, Shiming Li*, Wei Wei, Qingwang Liu, & Zengyuan Li. (2022). Natural Forest Gap Identification Based on Drone Lidar. Journal of Beijing Forestry University, 44(6): 44-53.

Summary

- Research activities of forest cover mapping, stress monitoring, parameter estimation.
- Exchange young scientists.
- More joint research and comparative studies.
- Wrap-up Dragon V outputs and apply Dragon VI.

[PROJECT ID. 59358]

[China-ESA Forest Observation]

Thank you!

The joint use of Chinese and European satellites

Reconstructed airborne reflectance data at different times

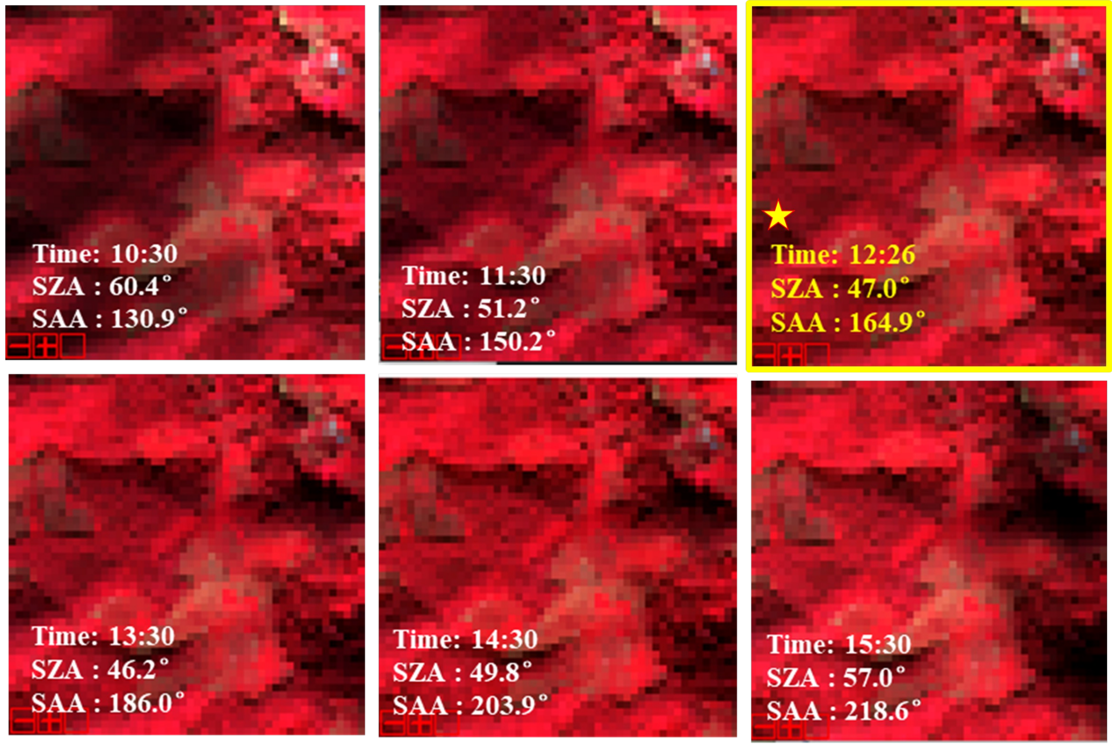

Validating GF-6 image NIR reflectance using reconstructed airborne imagery at different times

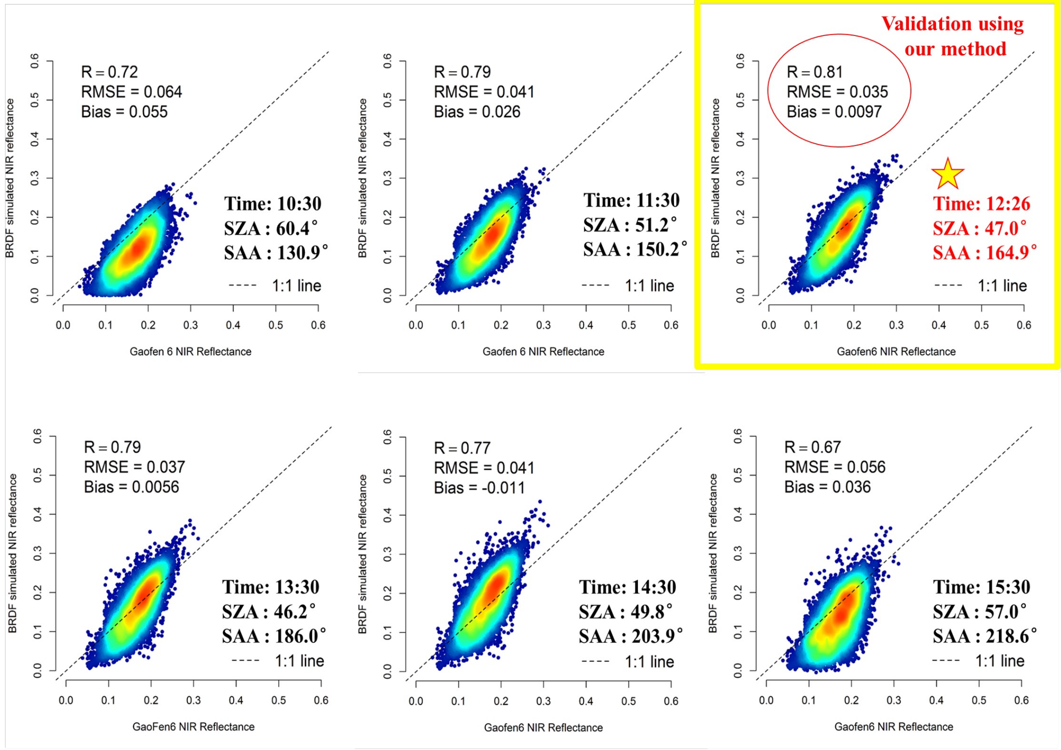

Instead of directly validating satellite data with airborne remote sensing data (NIR: R=0.80, RMSE =0.084, Bias=-0.07), the reconstructed airborne reflectance data (corresponding to the satellite imaging time) based on the BRDF model proves to be more efficient (NIR: R=0.81, RMSE =0.035, Bias=0.0097)for verifying satellite reflectance images in complex forested terrains.

Wen Jia, Yong Pang*. Satellite Reflectance Validation based on BRDF Reconstructed Airborne Hyperspectral Data.
Poster ID: 278 ; **Time:** Tuesday, 12/Sept/2023 4:09pm – 4:17pm; **Room:** 312 - Continuing Education College (CEC)

Forest carbon flux monitoring

- Flux tower in Puwen

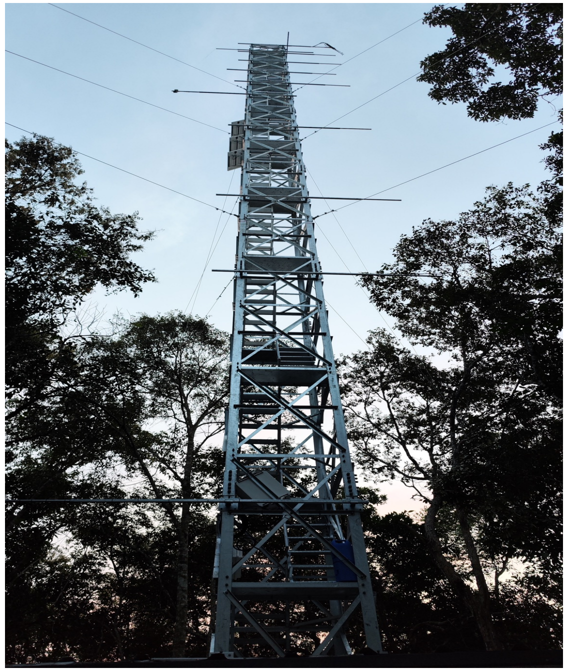

The flux tower is located in a tropical evergreen broad-leaved forest in Yunnan Province

Located at: 22°24 '59 "N,101°5' 25" E, altitude 960 m.

Tower is about 36 m tall.

The eddy covariance system includes a gas (CO_2/H_2O) analyzer (EC155) and a 3D ultrasonic wind speed sensor (CSAT3A).

Eddy covariance system

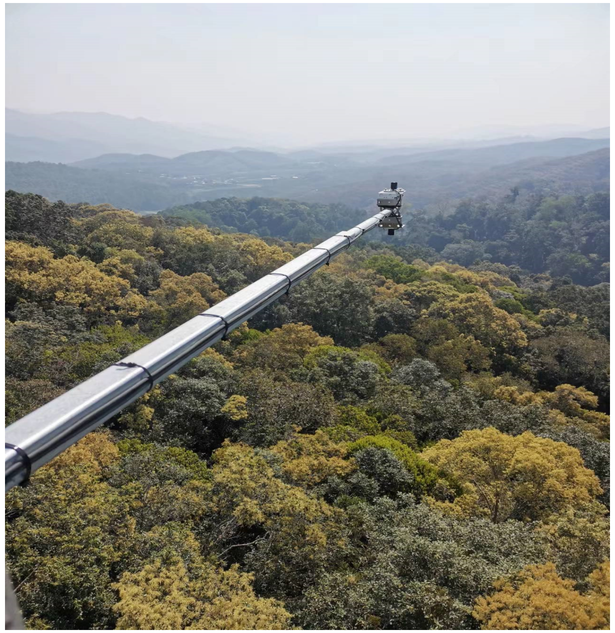

Sensor of photosynthetically

Forest carbon flux monitoring

■ An optimized method to validate high resolution gross primary production based on flux tower measurement

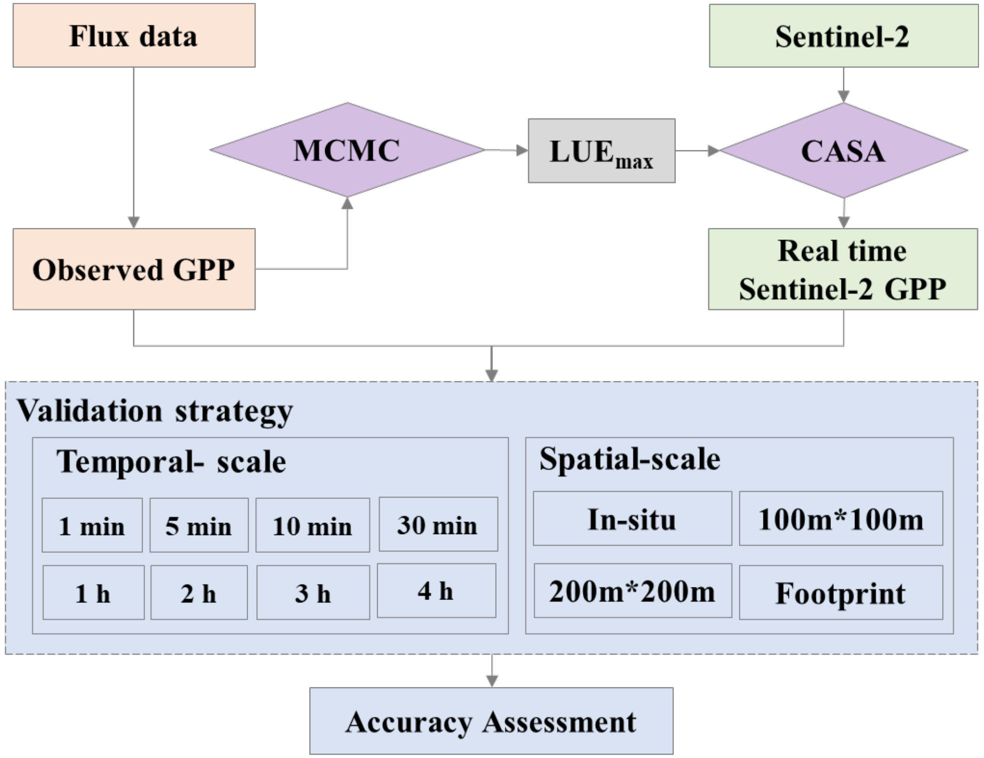

Flowchart of the optimized method to validation high resolution GPP

$$GPP = PAR \times FPAR \times \varepsilon_{max} \times f_1(T) \times f_2(\beta)$$

LUE_{max}： MCMC

Footprint model： Footprint Source Area Model, FSAM

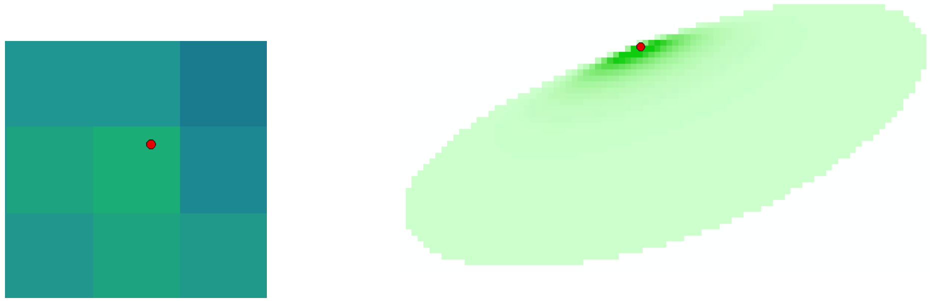

$$W = \frac{f(x,y,z_m)_i}{\sum_{i=1}^{N} f(x,y,z_m)_i} \times 100\%$$

$$GPP = \frac{\sum GPP_{i,j}}{n}$$

$$GPP_{footprint} = \sum W_{i,j} \times GPP_{i,j}$$

Tao Yu, Yong Pang*, Xiaodong Niu, Zengyuan Li. An optimized method to validate high resolution gross primary production based on flux tower measurement
Poster ID： 279； **Time:** Tuesday, 12/Sept/2023 4:17pm - 4:25pm; **Room:** 312 - Continuing Education College (CEC)

Forest carbon flux monitoring

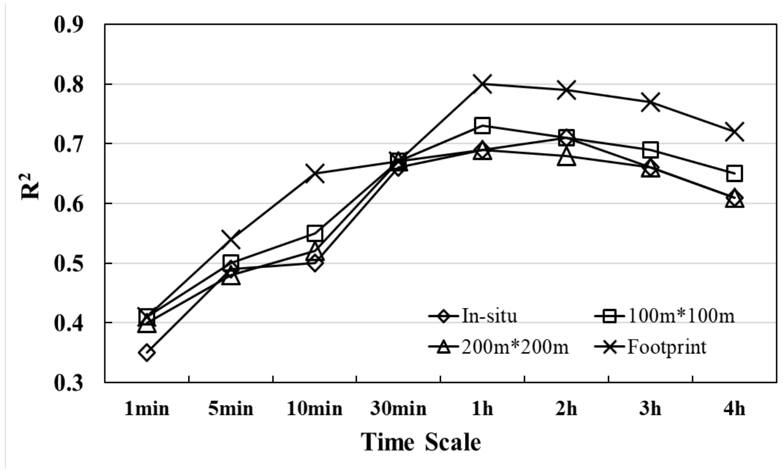

R^2 trend

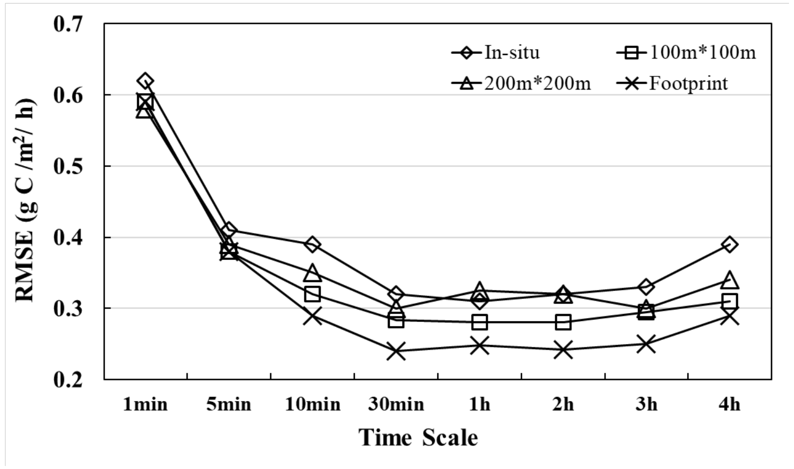

RMSE trend

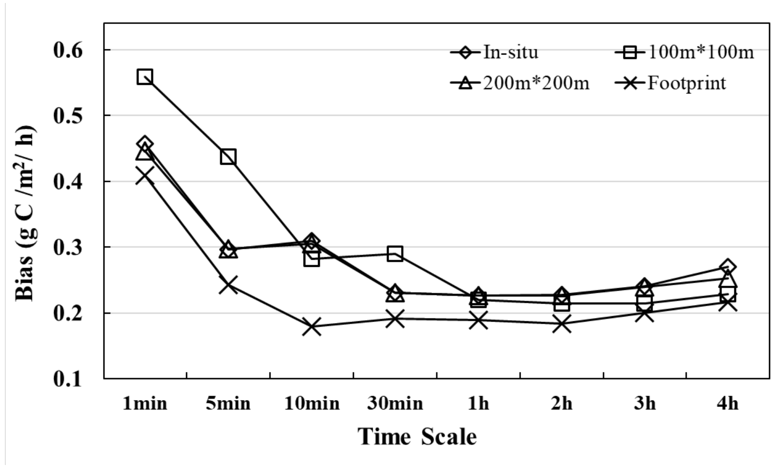

Bias trend

- Better linear relationships could be achieved between Sentinel-2 GPP and flux tower GPP when taking into account the footprint of flux data.
- Better correlation could be observed between Sentinel-2 GPP and flux tower GPP derived in 30min~2h of the satellite overpassing time.

Tao Yu, Yong Pang*, Xiaodong Niu, Zengyuan Li. An optimized method to validate high resolution gross primary production based on flux tower measurement
Poster ID： 279 ; **Time:** Tuesday, 12/Sept/2023 4:17pm - 4:25pm; **Room:** 312 - Continuing Education College (CEC)

Forest gap identification and aboveground biomass calculation based on multi-source LiDAR

AGB estimation using LBI (LiDAR biomass index)

$$LBI = \lim_{\Delta H \to 0} \sum_{H=H_c}^{H_T} U_L(H) \cdot [r(H)]^2 \cdot \Delta H \cdot H \qquad lnAGB = ln\kappa + \beta lnH_T + \frac{2\beta}{\alpha} lnLBI$$

***α*, β, κ** can be obtained by regression of a small amount of field measured data

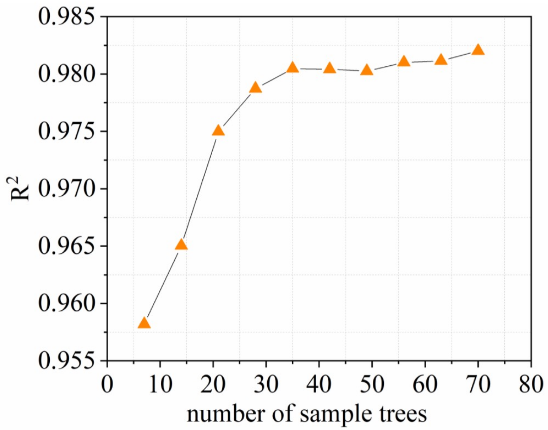

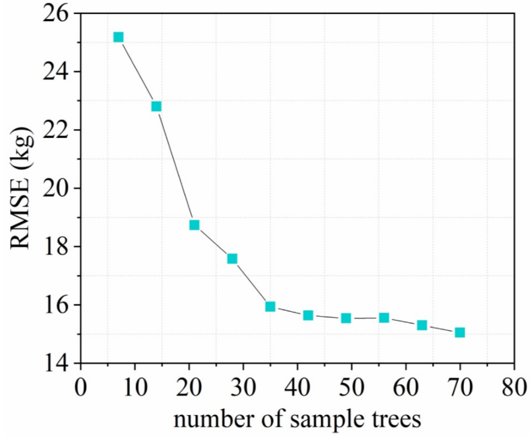

LBI can estimate the biomass of a large range of area by selecting a few sample trees (i.e., 35) to calibrate the model

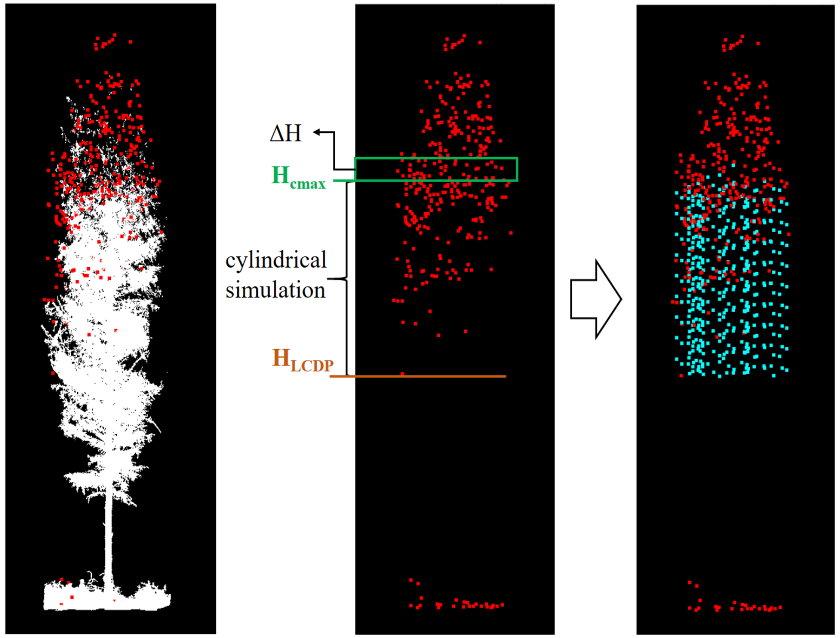

points compensation of individual tree

Main step:

- Points compensation
- LBI and tree height calculation
- AGB calculation

Liming Du, Yong Pang*. Potential Assessment of LBI for forest carbon sink measurement.
Poster ID: 275 ; **Time:** Tuesday, 12/Sept/2023 4.01pm - 4:09pm; **Room:** 312 - Continuing Education College (CEC)

Forest gap identification and aboveground biomass calculation based on multi-source LiDAR

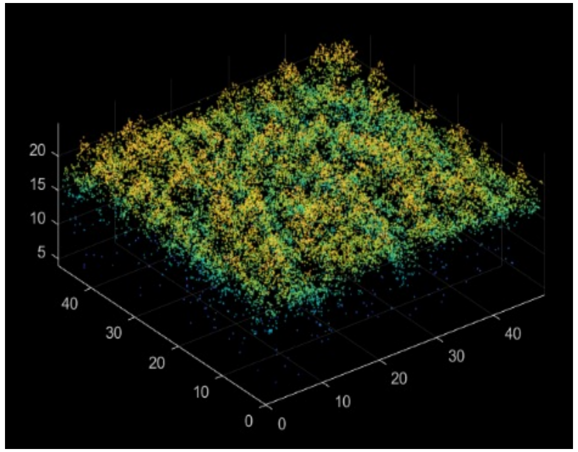

Individual tree segmentation

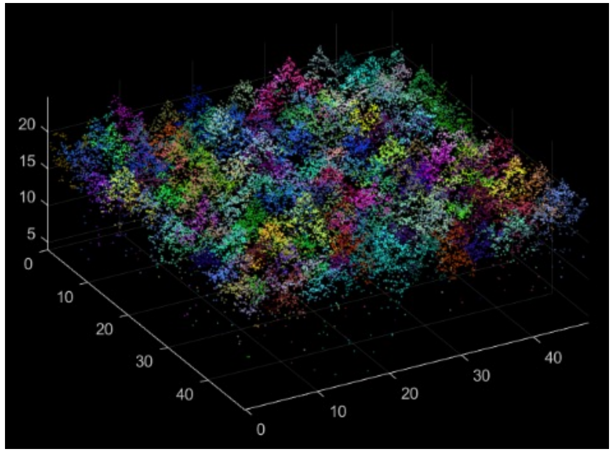

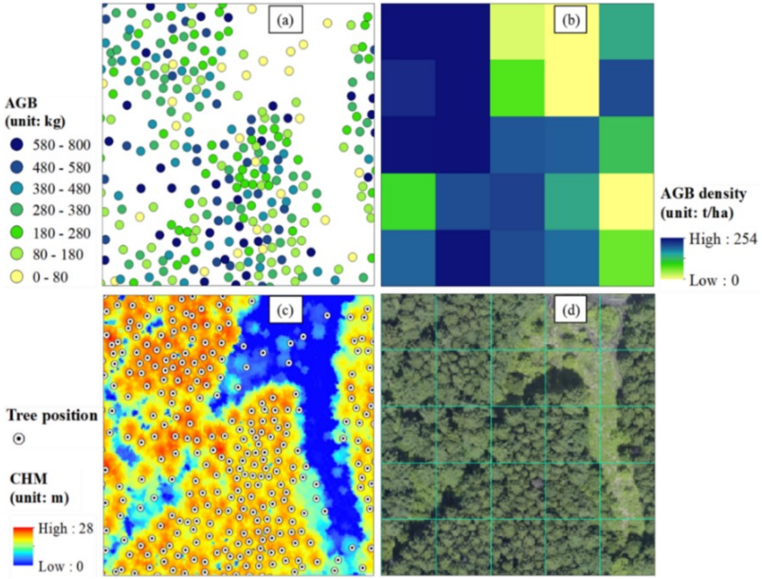

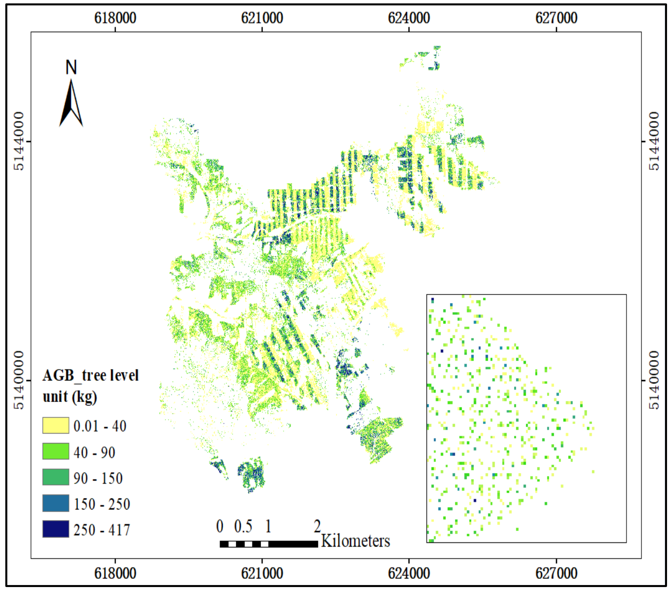

Liming Du, Yong Pang*. Potential Assessment of LBI for forest carbon sink measurement.
Poster ID： 275 ; **Time:** Tuesday, 12/Sept/2023 4.01pm - 4:09pm; **Room:** 312 - Continuing Education College (CEC)

Forest gap identification and aboveground biomass calculation based on multi-source LiDAR

■ AGB calculation of Pu'er based on TLS data

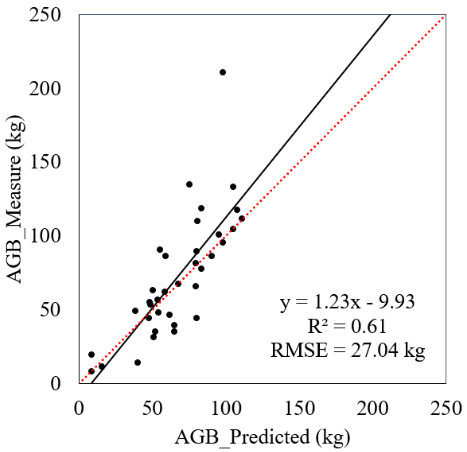

Modeling accuracy

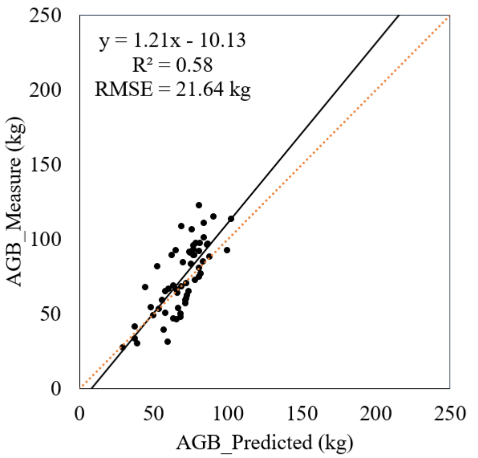

Accuracy verification (tree level)

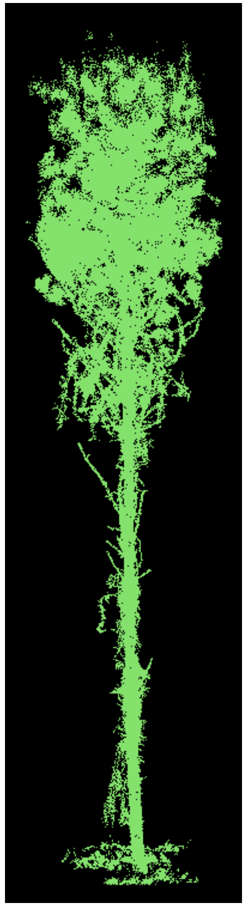

LBI
height
crown
First living branch height
Crown length
Crown volume
……

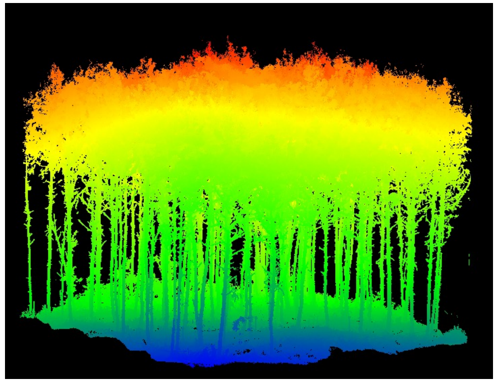

Original TLS data

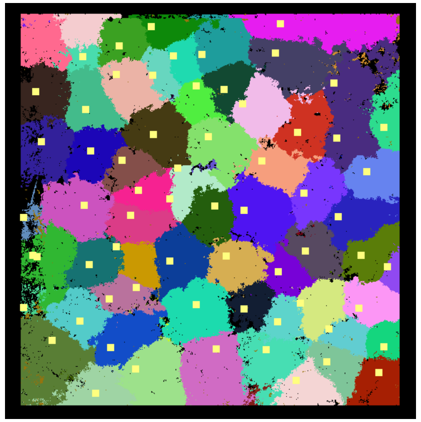

Individual Tree Segmentation result of TLS data

Liming Du, Yong Pang*. Potential Assessment of LBI for forest carbon sink measurement.
Poster ID： 275 ; **Time:** Tuesday, 12/Sept/2023 4.01pm - 4:09pm; **Room:** 312 - Continuing Education College (CEC)

Forest gap identification and aboveground biomass calculation based on multi-source LiDAR

- AGB calculation of Pu’er based on ALS data of 2018 and 2023

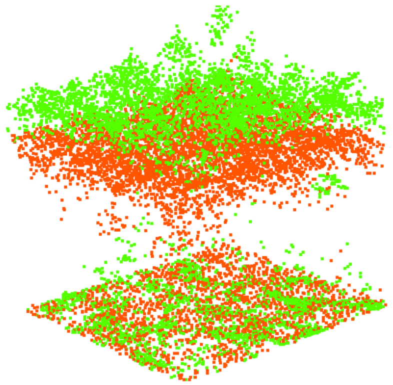

Green
ALS data of 2023

Red
ALS data of 2018

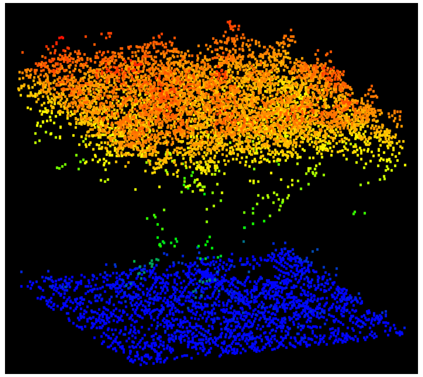

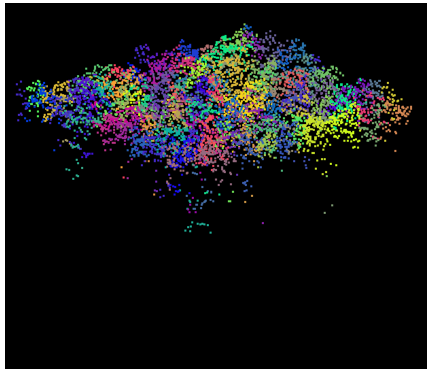

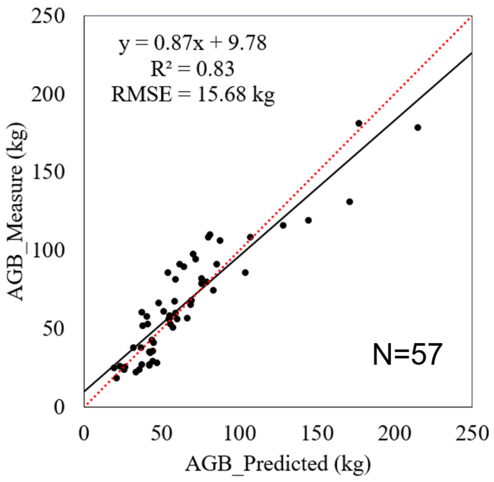

AGB_LBI model (2018)

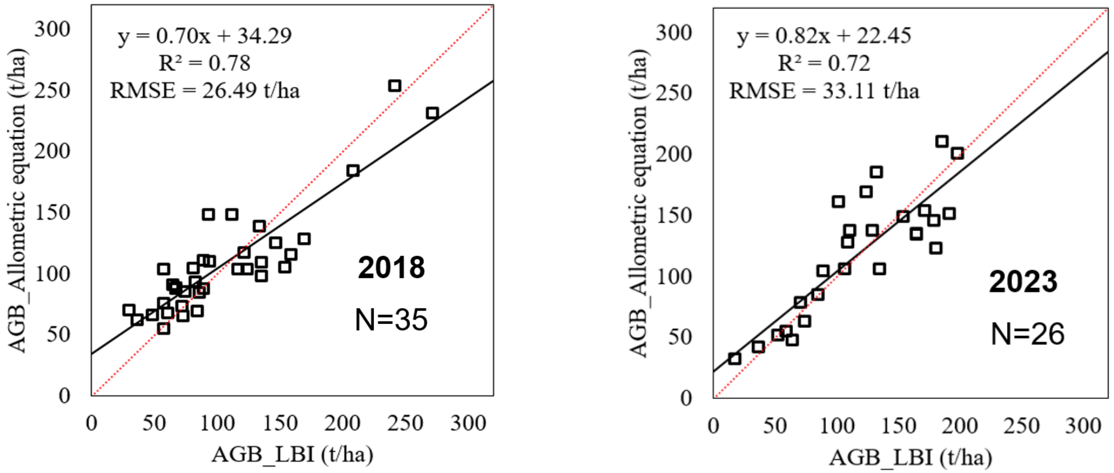

Plot level verification result of different years

Liming Du, Yong Pang*. Potential Assessment of LBI for forest carbon sink measurement.
Poster ID： 275 ; **Time:** Tuesday, 12/Sept/2023 4.01pm - 4:09pm; **Room:** 312 - Continuing Education College (CEC)